Multi-Proxy analysis in the Gangotri Glacier region, Garhwal Himalaya: Glacial Stratigraphy and the overview of snout retreat, geomorphic evolution, and palaeoclimate signatures

DHRUV SEN SINGH[1*], ANOOP KUMAR SINGH[1], CHETAN ANAND DUBEY[1], DHIRENDRA KUMAR[1],
SATISH JAGDEO SANGODE[2], ANJALI TRIVEDI[3], RAJESH AGNIHOTRI[3] & JAYENDRA SINGH[4]

JPSI

The dynamic behavior of glaciers in the Himalayan region produced the landforms, which provide valuable information on the long-term effects of climate change and landscape evolution. The Gangotri glacier, one of the most dynamic and relatively well-documented glacial system, is longest valley glaciers out of 968 glaciers scattered over the Uttarakhand Himalayan Range. Although extensive mapping has been carried out, the retrieved data set still lacks unanimous understanding on the pattern of retreat and also its geomorphic response. Furthermore, inadequate and isolated information from dendrochronology, sedimentology, mineral magnetism, palynology, black carbon deposition, geochronology and palaeoclimatic approaches preclude understanding on the chronologic correlation and glacial stratigraphy. However, climate change urgently demands in-depth information on flashfloods and such processes responsible for landscape modification.

The Gangotri glacier has experienced varying rates of retreat since 1935 from as low as 20 m/y, to very high rates of 30-50 m/y (1960 to 1990). During the last few decades, the rate is observed to be decreasing to 10-15 m/y (2015-2021). The geochronology based studies, indicated glacier terminus around 3.7 km down during ~200-300 yrs B.P from its position in 1992. This was clarified by tree colonization pattern study in the glacier forefields, which precisely established for the first time that the Gangotri glacier terminus receded only ~63 meters during 1571-1934 C.E. of total recede ~1.853 km in the past 447 years (1571 to July 2017).

The Gangotri Glacier Region (GGR) exhibits stratified as well as unstratified glacial and non-glacial landforms. The unstratified glacial deposits represent Lateral Moraines (LM) and Recessional Moraines (RM), whereas the stratified deposits occur as Outwash Plains (OWP) and Kame Terraces (KT). The non-glacial landforms are unstratified Debris Cones (DC), Pillar Structures (PS) and stratified Flash Flood Deposits (FFD). The sedimentary analysis describes that the OWP sediments are poorly sorted medium sand evolved by glacio-fluvial processes, whereas sediments of KT are well-sorted sand and silt evolved by a combination of two depositional environments, the glacio-fluvial at the base and lacustrine at the top.

Palynological analysis revealed the presence of pollen-spores of local terrestrial herbaceous as well as marshy taxa, along with temperate tree taxa, transported from lower altitudes in good amount during the Early Holocene. The carbon isotopic analysis indicated that the GGR is characterized by both C_3-C_4 i.e. mixed type of vegetation. The average value in the weight % of BC is 0.07 and the weight % of $\delta^{13}C_{BC}$ is -25.2‰, which is close to atmospheric aerosols containing vehicular emissions mainly during the common traffic (~ -26‰). The mineral magnetic analysis of KT reflects dominance of detrital influx depicting warm episodes having well-oxygenated ponding conditions that ended with restricted cold climatic events. A combination of geochronology, sedimentology and mineral magnetic studies were integrated with other proxies to build up the Late Quaternary stratigraphy in this region. Tributary glaciers, snow melt ephemeral streams, mass movements, landslide lake outburst flooding (LLOF), and glacier lake outburst flooding (GLOF) are considered as important phenomena, which affects the glacial signatures and creates vision in identification of the landforms. The modification of glacial landforms and landscape of GGR are the main reasons for diversified opinion on glacial history.

The geochronology of various sections of the glacial stratified deposits provide the record of climate change of last 25 Ka BP with major warm and cold events such as the Last Glacial Maximum (21-19.5 Ka BP), Older Dryas (16.5-14.5 Ka BP), Bølling-Allerød (14.5-13.5 Ka BP), Younger Dryas (13.5-12 Ka BP), Indus Valley Civilization Collapse (5.0-3.0 Ka BP), Medieval Warm Period (1.25-0.7 Ka BP) and Little Ice Age (0.7 -0.2 Ka BP). The geomorphic features such as Terminal Moraines (62.89±8.58 Ka BP), Oldest Lateral Moraines (~ 60 Ka BP), Oldest Outwash Plains (~ 60 Ka BP), Kame Terraces (25.0 - 0.3 Ka BP), Old Lateral Moraines (17.56±4.11- 4.84±1.21 Ka BP), Old Outwash Plains (5.13±1.54 - 3.3 Ka BP), Debris Cones (5.2- 1.8 Ka BP), New Lateral Moraines (1.0- 0.35 Ka BP) and New Outwash Plains (1.82 - 1.0 Ka BP) are the main glacial stratigraphic units and sequences.

This paper presents the glacial stratigraphy and the overview on geological analysis in the GGR in light of rate of retreat, dendrochronologic attributes, geomorphological imprints, sedimentologic signatures, mineral magnetic

response, palynological distribution, carbon deposition, flash floods events, processes of landscape modification, geochronology, and major climatic events, which may provide significant inputs in understanding other glaciated regions in the Himalaya.

*[1]Department of Geology, University of Lucknow, Lucknow-226007, India; [2]Department of Geology, Savitribai Phule Pune University, Pune-411007, India; [3]Birbal Sahni Institute of Palaeosciences, Lucknow-226007, India; [4]Wadia Institute of Himalayan Geology, Dehradun-248001, India. *Corresponding Author's e-mail: dhruvsensingh@rediffmail.com*

INTRODUCTION

The Himalaya is an abode of snow, ice, and glaciers. It is one of the most important regions outside the polar region to bear the glaciers. It contains about 9575 glaciers spreading over 43000 km² which varies in size from less than a km to as long as 72 km long Siachen glacier (GSI, 2009). Glaciers in the Himalaya are formed due to successive accumulation of snow over long period of time and have evolved in direct response to the climate and Himalayan orogeny. The distribution and style of glaciations throughout the Himalaya are strongly influenced by the SW Indian Monsoon, mid latitude Westerlies and El-Niño southern oscillation (ENSO) (Owen *et al.,* 1998). Rapid differential uplift of the Himalaya (Fort, 1995) and the Tibetan Plateau (Ruddiman and Kutzbach, 1991) during late Cenozoic times may also have been important in controlling the style of glaciations and the global climate. Sufficient snowfall, shady northern slopes, low temperature, and gentle slope gradient of the valley are the favorable conditions for glaciations over the Himalaya. The Gangotri is one of the longest valley glaciers of the Uttarakhand Himalaya. It is the birth place of the holy river Ganga, which serves as life line for millions of people of northern plains of India. Therefore, multi-proxy analysis and overview of the GGR is of prime importance.

The glacial fluctuations are considered as one of the most sensitive indicators of climate change. Retreat of several glaciers during past few decades is a clear sign of global warming (Porter, 1970; Mayewski and Jeschke, 1979; Ageta *et al.,* 2001; Singh *et al.,* 2017, 2019; Kumar *et al.,* 2017, 2020), in response to anthropogenic activities (Houghton *et al.,* 1990, 1996). Different rates of retreat of glacier and even advances in some regions indicate towards the differential response of the glaciers depicting complex geomorphic-sedimentological processes operating under various synoptic climatic regime. It illustrates that glacier dynamics is not only controlled by climate variations, but also depends upon glacier characteristics and local aspects. The retreat of the Gangotri glacier was so high in the past that the Intergovernmental Panel on Climate Change (IPCC) in 2007 in its 4th report predicted that the Gangotri glacier will disappear by 2035, which was retracted by the IPCC in January 2010. It has been pointed out that, it is difficult to establish why glaciers existing in similar climatic regime are responding differently to the same climate/environmental change (Raina, 2013), and why different workers have reported varied rate of retreat for the Gangotri glacier (Singh

and Mishra, 2001; Naithani *et al.,* 2001; Kar *et al.,* 2002; Singh and Mishra, 2002a; Singh, 2004, 2015; Yadav *et al.,* 2004; Bhambri *et al.,* 2012; Singh, 2013a; Singh *et al.,* 2017, 2019).

The Gangotri glacier has been analysed for the Quaternary glacial history (Sharma and Owen, 1996; Ali and Juyal 2013), fluctuations of glacier snout since 1935 by the Geological Survey of India, rate of retreat and shrinkage of glacier (Singh and Mishra, 2001; Bhambri *et al.,* 2012; Singh *et al.,* 2017), tree rings (J. Singh *et al.,* 2020), processes of sedimentation (Singh and Mishra, 2001), morphometry and morphotectonics (Naithani *et al.,*2001; Bali *et al,* 2003), vegetation based palaeoclimate (Kar *et al.,* 2002), role of tributary glaciers on landscape modification (Singh and Mishra, 2002 a,b), morpho-sedimentary processes (Singh, 2004), hydrological characteristics (Singh *et al.,* 2006), snow-melt ephemeral streams (Singh, 2013a), ice thickness (Gantayat *et al.,* 2014), monsoon variability and major climatic events (Singh *et al.,* 2019), mass movement (A.K. Singh *et al.,* 2020), recessional pattern of Thelu and Swetvarn glaciers (Kumar *et al.,* 2021a,b) etc.

All these studies, however, report a diversified opinion about climatic events, rate of retreat, and extent of former glaciations, mainly due to lack of geochronological data and misinterpretation of landforms (Benn and Owen, 2002; Singh and Mishra, 2002a). The coexistence of glacial and non-glacial geomorphic features and their modification suggest that the GGR is subjected to complex interplay of many processes.

Diverse inferences from the glaciated terrain in general and the Gangotri glacier in particular are the main reasons for re-examinations and generating more data set from the GGR. We provide glacial stratigraphy and the overview on various aspects of geology such as pattern of retreat, tree ring, geomorphology, sedimentology, geochronology, mineral magnetism, palynology, carbon deposition, landforms/ landscape modification, and major climate events.

STUDY AREA

The Gangotri glacier is situated between 30⁰44'-30⁰56'N latitudes and 79⁰04'-79⁰15'E longitudes in the Uttarkashi District of the Uttarakhand state. It originates from the Chaukhamba group of peaks at an elevation of about 6957 m msl and bordered by Satopanth and Bhagirath Kharak glacier
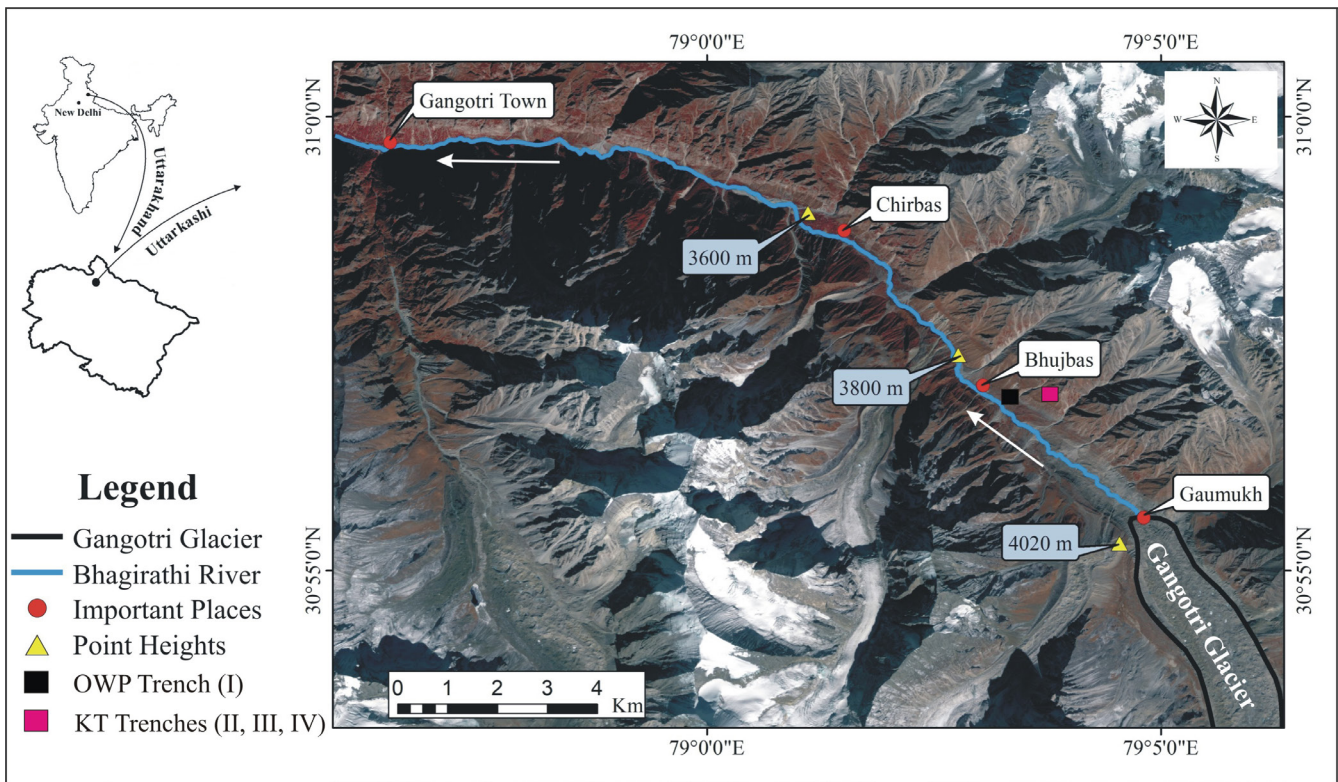
Fig. 1. Location map showing Gangotri glacier, Bhagirathi river, Gaumukh, Bhujbas, Chirbas, point heights and Gangotri town.

in the east, Chorabari glacier in the west, and Mandani Parbat in the south. It is about 30 km long and 0.5-2.5 km wide (GSI, 2009) flowing in the NW direction (Fig. 1). The Gangotri glacier has two principal areas, marked by the accumulation zone and ablation zone, separated by the equilibrium line. The ice melts continuously in the ablation zone so that the debris in this area increases and may eventually cover the glacier surface.

The Gangotri glacier is characterized by abundance of supraglacial moraines and their thick accumulation in the ablation zone. The ablation zone also exhibits small to large size open linear cracks known as crevasses, which are generally transverse on the surface and ranges from 3-10 m in length and 2-5 m in width (Singh and Mishra, 2001). In some of the openings, the melt water may accumulate to form supraglacial lakes. These lakes are more often formed in ablation area. The end point of the Gangotri glacier i.e. snout, known as Gaumukh, is at a distance of about 18 km from the Gangotri township. Gaumukh (an ice cave) is about 10-20 m in height and 15-30 m in width, which keeps on changing its shape and size every year. The Bhagirathi river originates from Gaumukh and is situated more towards left valley wall due to tilt of the valley.

The Gangotri glacier is a compound valley glacier, where many tributaries make their own contribution to the trunk stream. The SOI topographical sheets, Indian Remote Sensing satellite (IRS-1D), Linear Imaging Self Scanning Sensor data (LISS-III), and field observations show that numerous small sized valley glaciers designated as tributary glaciers feed and contribute into the main glacier to form the Gangotri group of glacier (Fig. 2). These tributaries are 3-20 km in length, which are generally transverse to the main

Table 1. Details of tributary glaciers of the Gangotri glacier.

Glacier/ bamak	Height (m)	Length (km)	Area (km²)	ELA (m)	Feeding Bank
Maiandi Bamak	5200-6300	5.0	6.0	5490	Right
Swachhand	4900-5800	8.0	17.5	5535	Right
Ghanohim	4800-6400	5.5	14.0	5290	Left
Kirti Bamak	4500-6800	8.0	24.0	5550	Left
Chaturangi Bamak	4400-5400	15.0	14.0	5180	Right
Meru Bamak	4300-5700	7.0	8.0	5260	Left
Raktavaran	4600-6000	15.0	19.0	5350	Right
Swetvarn Bamak	4800-5900	6.0	8.5	5340	Right
Bhrigupant Bamak	4000-6400	9.0	14.0	4900	Left
Manda Bamak	3800-5800	4.0	3.0	4600	Left
Matri bamak	4000-6400	3.5	4.0	5100	Right

glacier (Table 1). Due to the shrinkage and recession of the Gangotri glacier in time and space, few tributary glaciers detached from the main trunk glacier and thus became inactive (Singh and Mishra, 2002a).

RESULTS AND DISSCUSSION

Recessional pattern

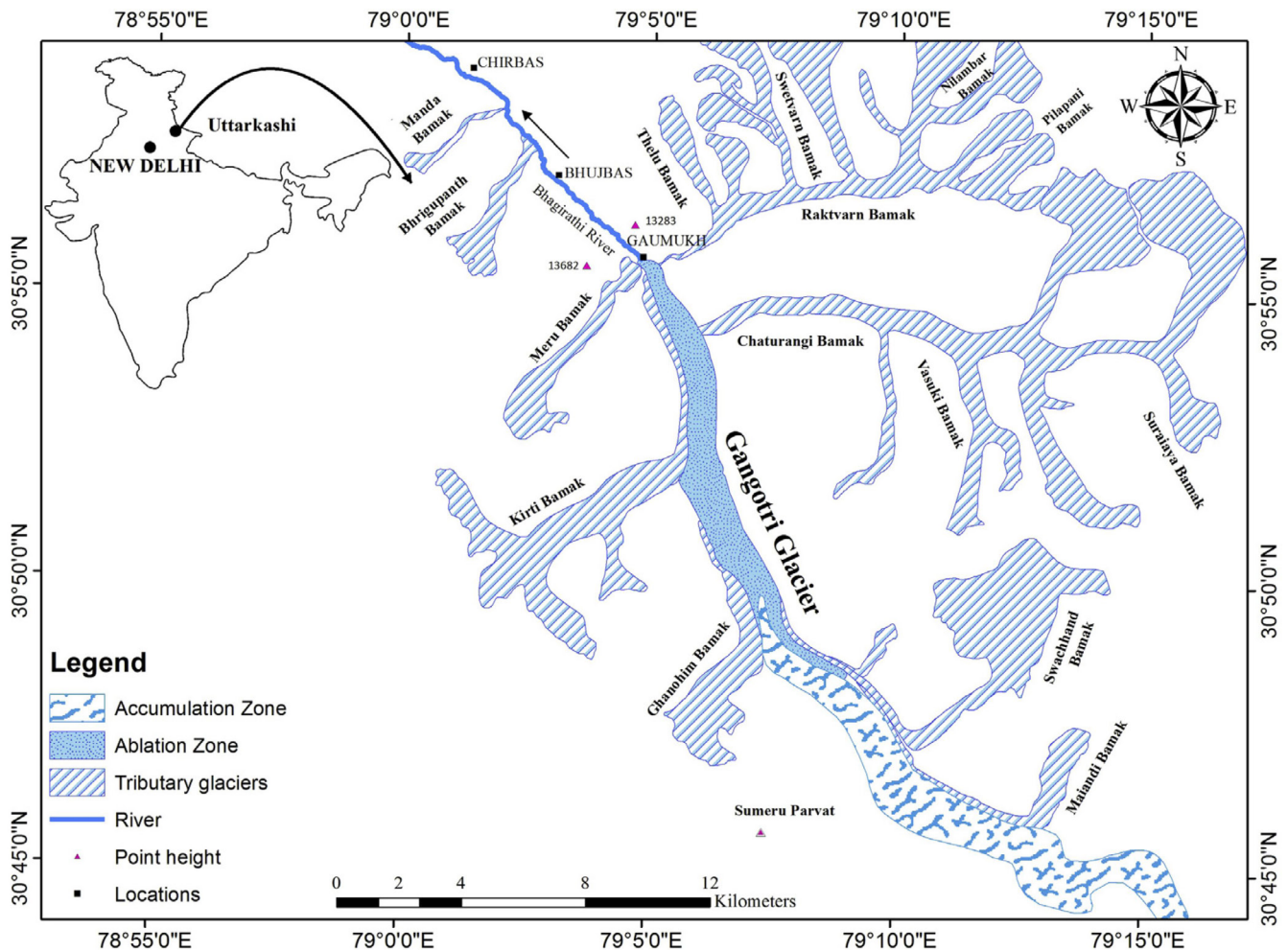Snout retreat is the direct and most important parameter

Fig. 2. Map showing Gangotri glacier and its tributaries, accumulation zone, ablation zone, Bhagirathi river, Bhujbas, Chirbas and few point heights (Singh *et al.,* 2017).

to understand global warming and climate change. The shrinking of the Gangotri glacier indicates that the area of cryosphere in GGR is decreasing. Survey of India toposheets of 1935 and 1962, and GSI expeditions provides the position of the snout of the Gangotri glacier. The increasing trend in retreat of the snout continued until around 1970. The remote sensing satellite data in conjunction with field investigations helped in precise monitoring of the snout. The rate of retreat of the snout of the Gangotri glacier using various methods by various institutions are presented in Table 2 and Fig. 3. It describes that the Gangotri glacier is retreating but the rate of retreat is generally decreasing contrary to the anthropogenically induced global warming (Singh *et al.,* 2017). The present study shows that the rate of retreat is 10.5 ma^{-1} between 2015 to 2021 (Table 2). More data set at annual resolution for a long period of time is required to understand the precise rate of retreat.

Further, if global warming is the only reason for the rapid rate of retreat of the Gangotri glacier then retreat rate for all the glaciers located in a similar climate regime should be uniform. However, a diverse rate of retreat has been noticed in glaciers and some glaciers are advancing too, which supports the view that other factors also control the glacier dynamics

Table 2. Rate of retreat of Gangotri glacier snout from 1935 to 2021.

Time period	Annual snout retreat (m)	Reference
1935-1956	10.16	Jangpangi (1958)
1956-1971	27.33	Vohra (1971)
1971-1974	27.34	Puri and Singh (1974)
1974-1975	35	Puri (1984)
1975-1976	38	Puri (1984)
1976-1977	30	Puri (1984)
1977-1990	28.08	Puri (1991)
1990-1996	28.33	Sangewar (1997)
1935-1996	18.8	Shankar and Srivastava (1999)
1962-1982	40	Tangri (2002)
1990	37	Tangri (2002)
1999	25	Tangri *et al.* (2004)
2004-2005	12.1	Kumar *et al.* (2008)
2013-2014	9.8	Bhattacharya *et al.* (2016)
1935-1976	23.95	Singh *et al.* (2017)
1976-1990	17.44	Singh *et al.* (2017)
1990-2001	12.55	Singh *et al.* (2017)
2001-2005	10.14	Singh *et al.* (2017)
2005-2012	11.48	Singh *et al.* (2017)
2001-2015	10	Singh *et al.* (2017)
2015-2021	10.5	Present Study
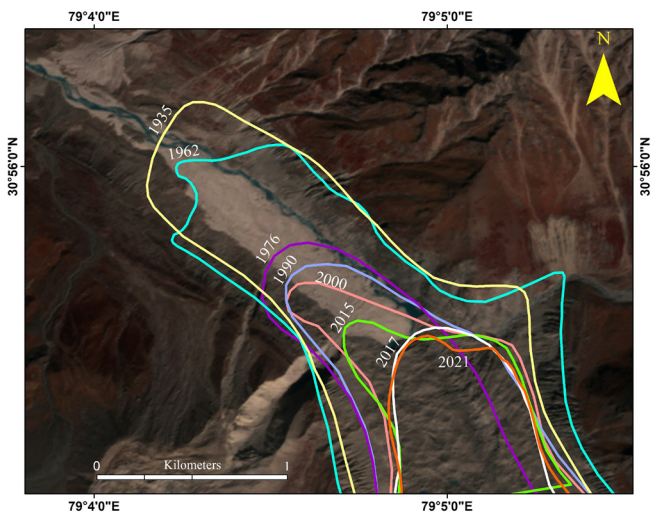
Fig. 3. Showing pattern of retreat for Gangotri glacier in different time interval from the year 1935 - 2021.
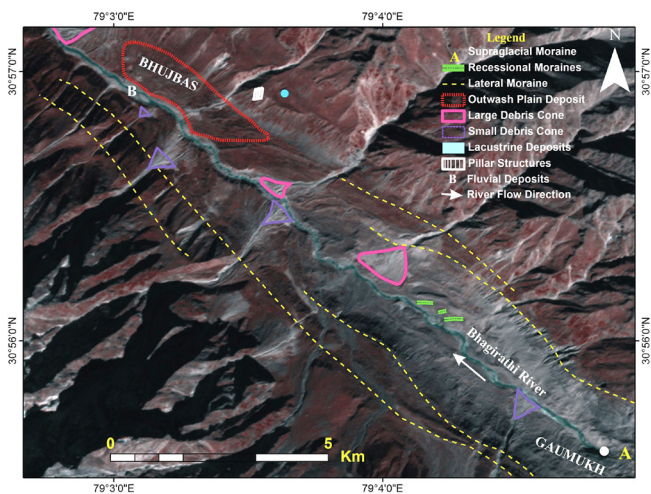
Fig. 4. Geomorphic map of the GGR showing glacial and non glacial landforms.

(Singh and Mishra, 2001). Other repositories such as tree ring based spring temperature records from the Garhwal Himalaya also showed the decrease in mean spring temperature since 1970 due to increase in diurnal range (Yadav *et al.,* 2004), which is again contrary to global warming. The recession of the Himalayan glaciers in response to anthropogenically induced global warming is still debatable (Armstrong, 2010, Bali *et al.,* 2011, Fujita *et al.,* 2008, 2009, Raina, 2009). In the Himalaya, monitoring of 2018 glacier snouts using satellite data from 2000/01/02 and 2010/11 shows that 1752 glaciers are stable having no change in the snout positions, while 248 glaciers are retreating and 18 of them are advancing (Bahuguna *et al.,* 2014).

Dendrochronology

Himalayan birch (*Betula utilis*) and Himalayan pine (*Pinus wallichiana*) ring-width chronologies as well as the colonization pattern of Himalayan birch growing in the Gangotri glacier forefield precisely established its terminus dynamics for the first time back to 1571 C.E. (J. Singh *et al.*, 2020). The Glacier terminus estimation was done using Himalayan birch colonization pattern study. The oldest age of Himalayan birch saplings/trees growing in the glacier forefield were considered to estimate the seedling/tree establishment year and distance from the terminus was used to estimate the terminus position in the past years. The study showed that Himalayan birch forest (established in year 1571 C.E.) is located 3.26 km away from the recent position (i.e. July, 2017) of the glacier terminus. It is worth noting that sapling can only be established when terrain was snow/ice free much before and sufficient organic matter was available for the establishment of the seedling. Study further revealed that Gangotri glacier terminus was ~1.853 km down steam from its recent position (i.e. July, 2017) in the late 16th century (1571 C.E.). However, earlier studies stated expansion of the Gangotri glacier (Bhujbas Stage) taken place ~440-210 yrs BP (1510-1740 C.E.) when it advanced ~3.7 km (with respect to the observations made in 1992) and remained stationary at Bhujbas for at least 200 years before it began to retreat in the late 19th century (Sharma and Owen, 1996; Srivastava, 2012). The cosmogenic radio-nuclide (CRN) dates also showed ~200-300 yrs BP (1750-1650 C.E.) age for the Bhujbas Stage of the Gangotri glacier expansion (Barnard *et al.*, 2004).

The colonization pattern of Himalayan birch has precisely revealed that the terminus receded ~1.853 km since 1571 C.E. The major part of which (1.79 km) receded since 1935 C.E., the glacier net retreat during 1571-1934 C.E was only ~63 meters. This also indicated that the glacier was almost stationary during 1571-1934 C.E and retreat got accelerated since 1957 C.E. (1.567 km). The Himalayan pine chronology representing October-November-December mean temperature also showed low radial growth during the late 17th- early 18th, late 18th-early 19th, 1860s and early 20th century pointing out cool phases supporting the stable conditions of the glacier. However, ring-width indices increased since the mid-20th century when retreat of the Gangotri glacier also gained pace (J. Singh *et al,.* 2020).

Geomorphology

Every landforms and associated depositional sedimentary environment has specific place, process, medium, and material of deposition (Singh, 2004) with definite accommodation space and supply of sediments. The nature of landforms depends upon the (a) supply of sediments (b) process of transportation and deposition of sediments and (c) availability of accommodation space for deposition. The geomorphic features of this region can be broadly classified into two, glacial landforms, which may be stratified and/or unstratified and non-glacial landforms. A geomorphic map of the GGR was prepared using remote sensing satellite data and field evidences (Fig. 4) and after analyzing all landforms a geomorphic model of the GGR was proposed (Fig. 5)

Glacial Landforms

The accommodation space for the evolution of landform is provided by the shrinking and retreating Gangotri glacier (Singh, 2004; Singh *et al.,* 2017) which vacates the valley. Sediments/debris are produced by the denudational processes on the rock wall and valley sides, that rise above the glacier surface or from erosion of the sub-glacial bed (Reading, 1986). The sediments produced by denudation are coarser and angular, whereas those produced by erosion of sub-glacial beds are finer, sub-rounded and striated.

The sediment/debris may be deposited to form different type of tills. The tills deposited in front and sides of a glacier known as moraines, are the most prominent depositional feature in a glaciated terrain. The glaciated regions are characterized dominantly by the presence of boulders with great variation in their size. Therefore, for better understanding of geomorphology and sedimentology in a glaciated terrain, these boulders are sub-divided into three categories (a) small size boulders varying in size from 25 - 60 cm (b) intermediate size boulders varying in size from 60 - 150 cm and (c) large size boulders > 150 cm.

Glacial unstratified deposits

Terminal/Recessional Moraines (TM/RM)

TM are ridges of unconsolidated debris deposited at the end margin of the glacier, which reflect the shape of the glacier terminus and also mark the maximum advance of the glacier. It is deposited in front of the glacier during stand still phase, when the melt rates were roughly equal to the flow from the glacier source.

TM/RM are observed as transverse ridges running across the valley, left as a glacier pauses during its retreat and indicate the temporary halt of a glacier. At least three stages of RM are present between Bhujbas and snout. A series of recessional morainic ridges lying between 900 m to 1400 m downstream of the recent snout (4,023 m) indicate the various stages of recession of the Gangotri glacier in the past (Singh *et al.,* 2017) (Fig. 6a). These RM are equivalent to the LIA 300-200 BP (Sharma and Owen, 1996; Singh *et al.,* 2019). TM are the first formed landforms in the GGR, and are considered up to Jhala, 40 km downstream to the Gangotri township around 63 Ka BP (Sharma and Owen, 1996).

Lateral moraines (LM)

The till deposited as parallel high ridges along the sides/ lateral margin of a glacier are known as lateral moraines. These landforms provide information about the palaeodynamics of the glacier. The LM indicating the shrinking of the Gangotri glacier are present on both sides of the Bhagirathi valley (Fig. 6b) from Gaumukh to Gangotri Township and further downstream. The distance between two successive moraines are high at the right bank and low at left bank. At least three major stages of LM can be identified on left valley wall, at an elevation of 5100, 4900, 4700 masl which are about 60-80, 40-50, 20-25 m higher than the present day Bhagirathi valley
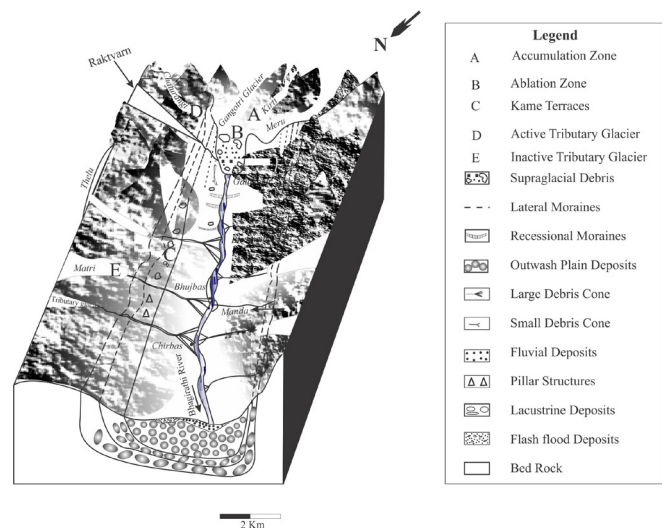

Fig. 5. Schematic geomorphic model of the GGR showing all glacial and non glacial landforms (modified after Singh, 2004).

respectively (Singh *et al.,* 2017). The maximum extent of the Gangotri glacier occurred around 63 ka BP known as Bhagirathi Glacial Stage, then Shivling Glacial advance during mid Holocene (< 5 Ka BP), and the Bhujbas Glacial advance about 200 to 300 BP (Sharma and Owen, 1996).

The oldest moraines might have been modified/washed out/eroded due to unstable slope gradient and the paraglacial processes. Morainic material in the form of isolated hillocks of unconsolidated material with boulders, cobbles and pebbles are abundantly found between snout and the Bhujbas. These hillocks known as hummocky moraines, are about 5-15 m above the present valley floor (Singh *et al.,* 2017). The oldest lateral moraine, old lateral moraine and new lateral moraine were evolved during ~ 60Ka BP, 17.56 - 4.84 Ka BP and 1.0-0.35 Ka BP (Barnard *et al.,* 2004) respectively.

Glacial stratified deposits

Outwash Plain Deposit (OWP)

Outwash plain also known as sandur deposits are formed beyond and in front of the snout of a glacier by melt water stream (Fig. 7a). Glaciers contain huge amount of debris and deposit it on a broad plain, when they are stagnant for a long period. Such deposits are sorted or graded into sizes by fluvial action, the coarsest near the ice, becoming progressively finer in the downstream direction. Thus, outwash plains are glacio-fluvial deposits similar to those of braided stream humid alluvial fans in which stratification is common due to fluvial action. OWP deposits are formed after RM and LM. The oldest OWP, old OWP and new OWP were evolved during the ~ 60Ka BP, ~ 5 Ka BP (Sharma and Owen, 1996) and 1.82-1.0 Ka BP (Barnard *et al.,* 2004) respectively.

Kame Terraces (KT)

Trough/depression is formed between the LM and the valley wall (Hewitt, 1993). The action of melt water streams
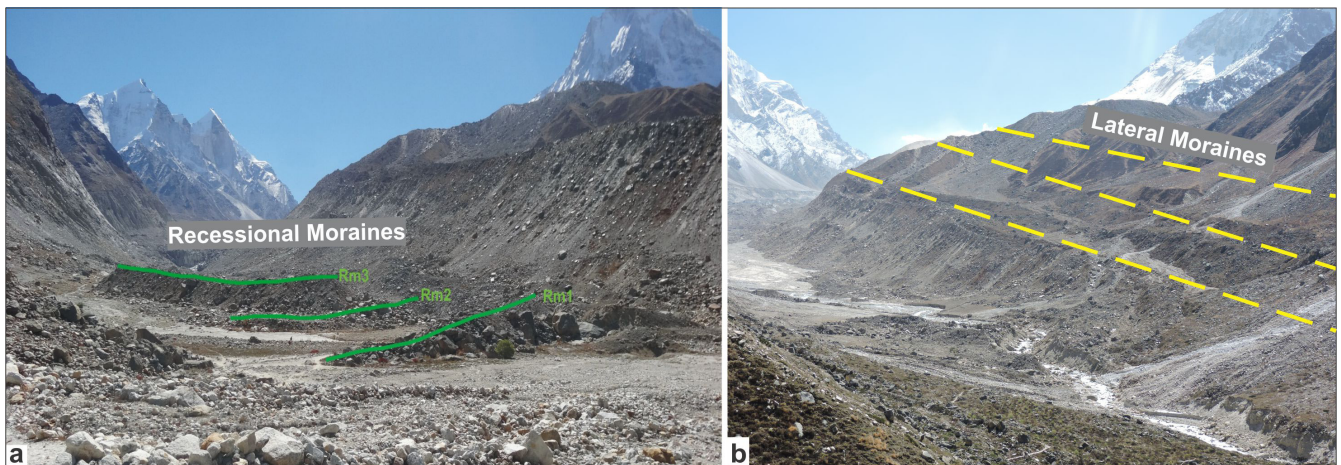
Fig 6. (a) Showing positions of different stages of recessional moraines indicating retreat of the Gangotri glacier; (b) temporal and spatial positions of three main stages of lateral moraines and so the shrinking of the Gangotri glacier.
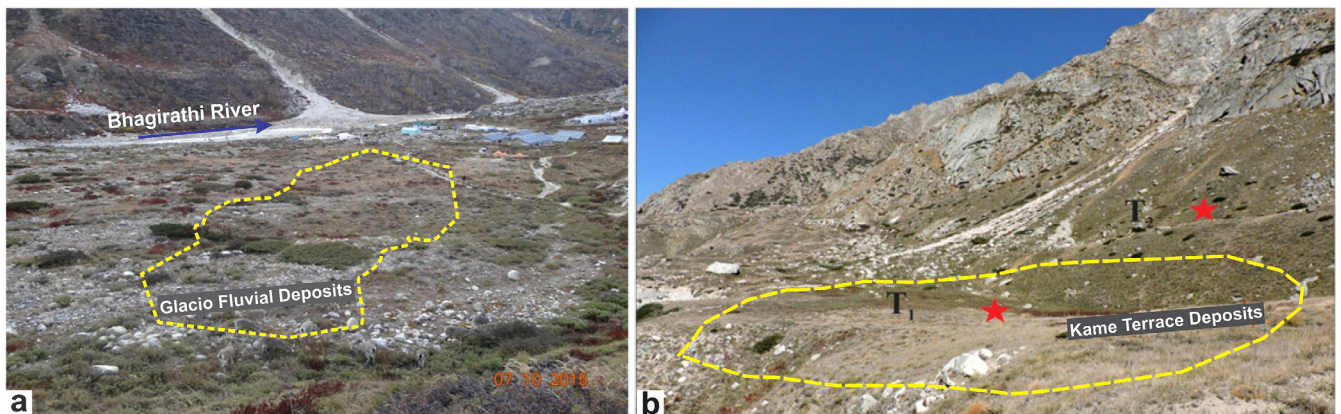

Fig. 7. (a) The photograph showing a. Bhagirathi river and glacio-fluvial deposits (Outwash Plain); (b) The photograph showing kame terraces.

that flow along the sides of a glacier, traps the glacio-fluvial sediments in this long depression/trough. The water in this depression is similar to a lake in which sediments have been transported by water. The filling of this trough/basin form a terrace, a flat region known as kame terrace (Fig. 7b). The lithologs explain that kame terraces are combination of two landforms, the LM at the base and lacustrine deposits at the top. The kame terrace deposits are basically the lake deposits above LM or between the LM and the valley wall (Singh *et al.,* 2019). The kame terraces are located at 150-300 feet higher elevation than the present day Bhagirathi river. The KT were evolved around ~ 25 Ka BP (Singh *et al.,* 2019; Dubey *et al.,* 2022).

Paraglacial landforms

Debris Cones (DC)

Recession of the Gangotri glacier vacates the Bhagirathi valley and provides the accommodation space for the mass movement. The tongue like features of debris with a surface slope greater than 10^0, which may be conical, triangular, fan or delta in shape, are known as talus cones or debris cones.

It is a prominent geomorphic unit which is well developed in the upper part of the Bhagirathi valley, upstream of the Gangotri township. These mass movement deposits show moderate grading from bottom to top in which coarser sediments are deposited at the base and finer at the top. Two types of debris cones are recognized in GGR (a) small debris cone and (b) large debris cone. Debris cones (5.2-1.8 Ka BP) are the youngest paraglacial landforms (Barnard et al., 2004).

Small Debris Cone (SDC)

Small debris cones, generally present on the left bank of the valley wall are formed as scree deposits by the rock fall. They occur as talus cone near the intersection of the valley wall with the valley surface (Fig. 8a). These are 5-25 m in length and 5-10m in width which slopes at a steep gradient.

Large Debris Cone (LDC)

The large debris cones are common on the right bank of the Bhagirathi valley and formed by debris flow. They originate at higher elevation on the valley wall and extend up
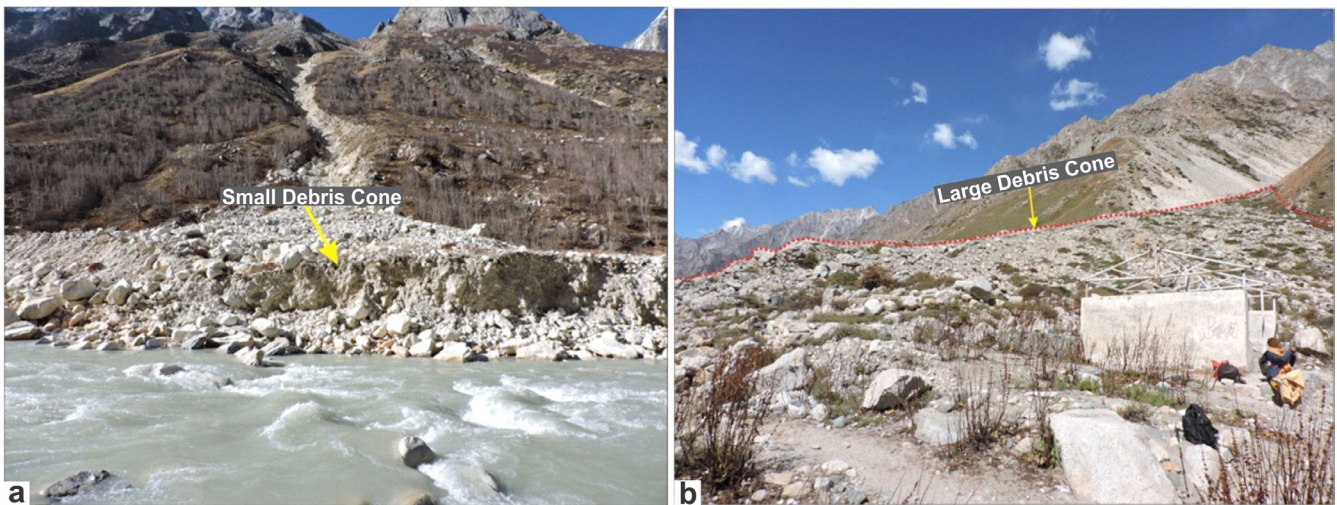
Fig. 8. (a) Small Debris Cone present on the left side of the Bhagirathi Valley; (b) Large Debris Cone present on the right side of the Bhagirathi Valley.
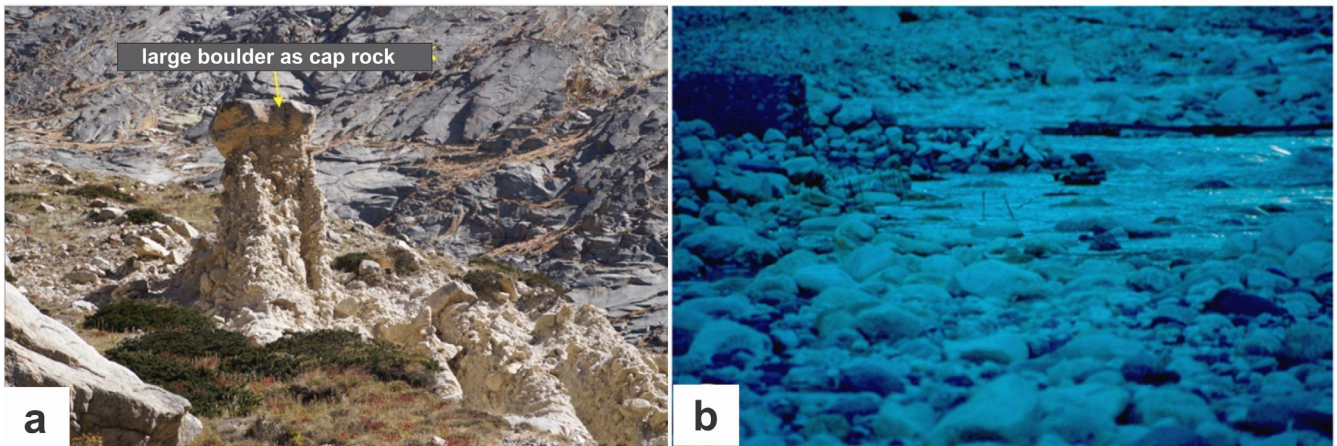

Fig. 9. (a) Pillar structure present in the upstream portion of the Gangotri glacier valley; (b) Flash Flood Deposits (remnant iron rods showing 1-1.5 m thick sedimentation within few hours) present in the upstream portion of the Gangotri glacier valley.

to the Bhagirathi river. Generally, LDC are absent on the left bank due to steep slope gradient and lack of accommodation space. At many places these debris cones have forced the Bhagirathi river to shift and have thus affected the sinuosity of the river up to some extent. The right bank debris cones are large because of the gentle slope gradient of the valley wall, which provide the accommodation space, and huge supply of sediments from the tributary glaciers. It is 50-100 m in length and 25-75 m in width (Fig. 8b).

Pillar Structures (PS)

The pillar structures are standing portion of poorly sorted materials consisting of clay to boulder size sediments, which are 1-5 m in height and 0.5-1 m in width. The term pillar structures have been preferred because they look like a pillar. The LM are breached by pluvial, aeolian, fluvial action and also by gravity fall. These structures are present only at the right bank of the valley between the first and third stages of the LM near Bhujbas, Chirbas and also at few other places. They are absent on the left bank due to the steep slope

gradient of the left valley wall (Singh, 2004).

In the moraines, heavy boulders are bypassed during erosion by rain, wind and ephemeral streams, (Singh, 2004; Singh *et al.*, 2017). These boulder cap protect the fine grained sediments lying below it from removal and thus the poorly sorted sediments remain as pillar structure with a boulder cap (Fig. 9a). Later, the cap boulder falls and the fine materials of the pillar structures are also removed and washed out completely. The lithological analysis and location of the pillar structures within the morainic ridges explain that pillar structures are secondary landforms formed by differential erosion of the pre-existing morainic ridges.

Flash Flood Deposits (FFD)

Heavy rain in a glaciated terrain fills the glacial lake and induces landslides. The landslides, block the river and may form the ephemeral lakes. The incessant rain overfills and causes bursting of ephemeral lakes and the glacial lakes, which creates LLOF and GLOF. The flooding redistributes huge amount of sediments and thus affects the pre-existing
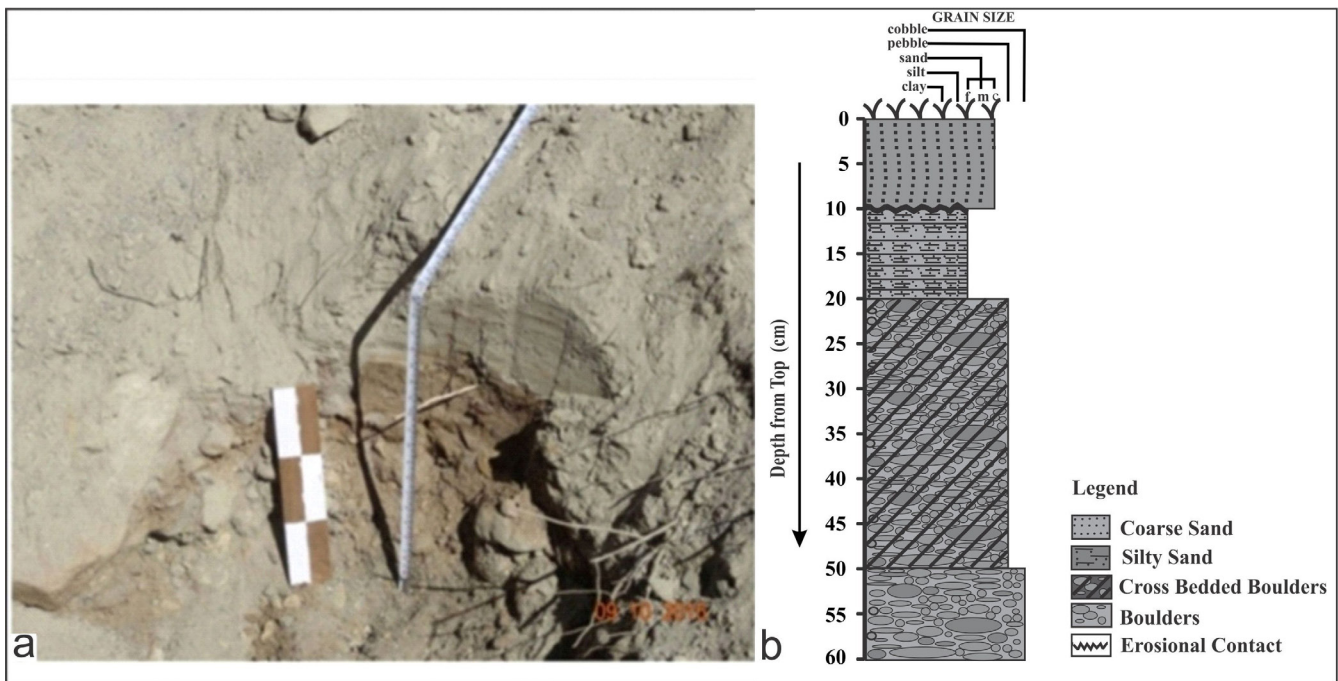
Fig. 10. (a) Photograph showing Trench I; (b) its Litholog in the outwash plain deposits.

landforms/landscape. In the GGR flash flood deposits (Singh and Mishra, 2002a) resulted due to LLOF on 6th June 2000, which redistributed huge amount of sediments in the Bhujbas area (Fig. 9b). LLOF and GLOF were reported again from the Kedarnath region also (Singh, 2013b, 2014). Poorly sorted thick accumulation of sediments are deposited within few hours (Singh and Mishra, 2002a; Dobhal *et al,* 2013; Singh, 2013b, 2014; Srivastava *et al.,* 2017) due to LLOF and GLOF.

Sediment grain parameters

Trenches were made and samples were collected in the stratified deposits for granulometric analysis at many places in the KT and OWP. Grain size provides fundamental information on the sedimentary processes, textural characteristics and hence the energy conditions of the depositional environment.

Outwash plain deposits

The sediment grain parameters such as mean grain size (M_Z), inclusive graphic standard deviation (σ_1), skewness (Sk_1) and kurtosis (K_G) of the OWP deposits are shown in Table 3 and Fig. 11. The M_Z varies from 0.25 Φ to 3.52 Φ; inclusive graphic standard deviation (σ_1) a measure of sorting, varies from 0.98 Φ to 1.68. The sediments are medium sand (Fig. 10 a), which are poorly sorted. It explains low to moderate energy of the depositional environment for long period with fluctuating energy conditions. Average value of inclusive graphic skewness (Sk_1) is 0.31 Φ i.e. positively skewed and value ranges from 0.07 Φ to 0.42 Φ i.e. from symmetrically skewed to very positively skewed, which explains that the finer sediments are in excess. Graphic kurtosis (K_G) ranges

between 0.78 Φ to 1.06 Φ i.e. from platykurtic to mesokurtic, explaining predominance of finer sediments. Table 4 shows the weight percentage of various grain size fractions at different locations in the OWP.

Table 3. Grain size parameters of outwash plain deposits.

Sample Number	M_Z (Φ)	σ_1 (Φ)	Sk_1 (Φ)	K_G (Φ)
GBO15 1	1.07	1.61	0.32	0.86
GBO15 2	2.87	1.22	0.09	0.79
GBO15 3	3.52	0.98	0.07	0.78
GBO15 4	1.37	1.62	0.14	0.83

Table 4. Weight percentage of various grain size fractions for the outwash plain.

Sample Number	V. C. Sand	C. Sand	M. Sand	F. Sand	V. F. Sand	Silt
GBO15 1	29.9	26.3	15.9	13.1	8.7	6.2
GBO15 2	-	-	27.6	27.6	24.8	20.0
GBO15 3	-	-	-	33.9	33.3	32.8
GBO15 4	22.5	22.4	20.0	17.4	11.3	6.4

The sediments of OWP deposits consist of a unimodal mixture of sand and silt. The unimodal nature of distribution may result from a single source of sediment transportation and deposition. The outwash plain deposits are stratified, consolidated to semi consolidated, coarse to fine grained sand and silt with boulders and shows primary sedimentary structures. The presence of ripples explains fluvial activity and the rounded gravels describe the medium degree of transportation from the place of weathering. Thus it can be inferred that the sediments of the OWP may have been deposited by the fluvial streams originating from the melting of glacial ice.
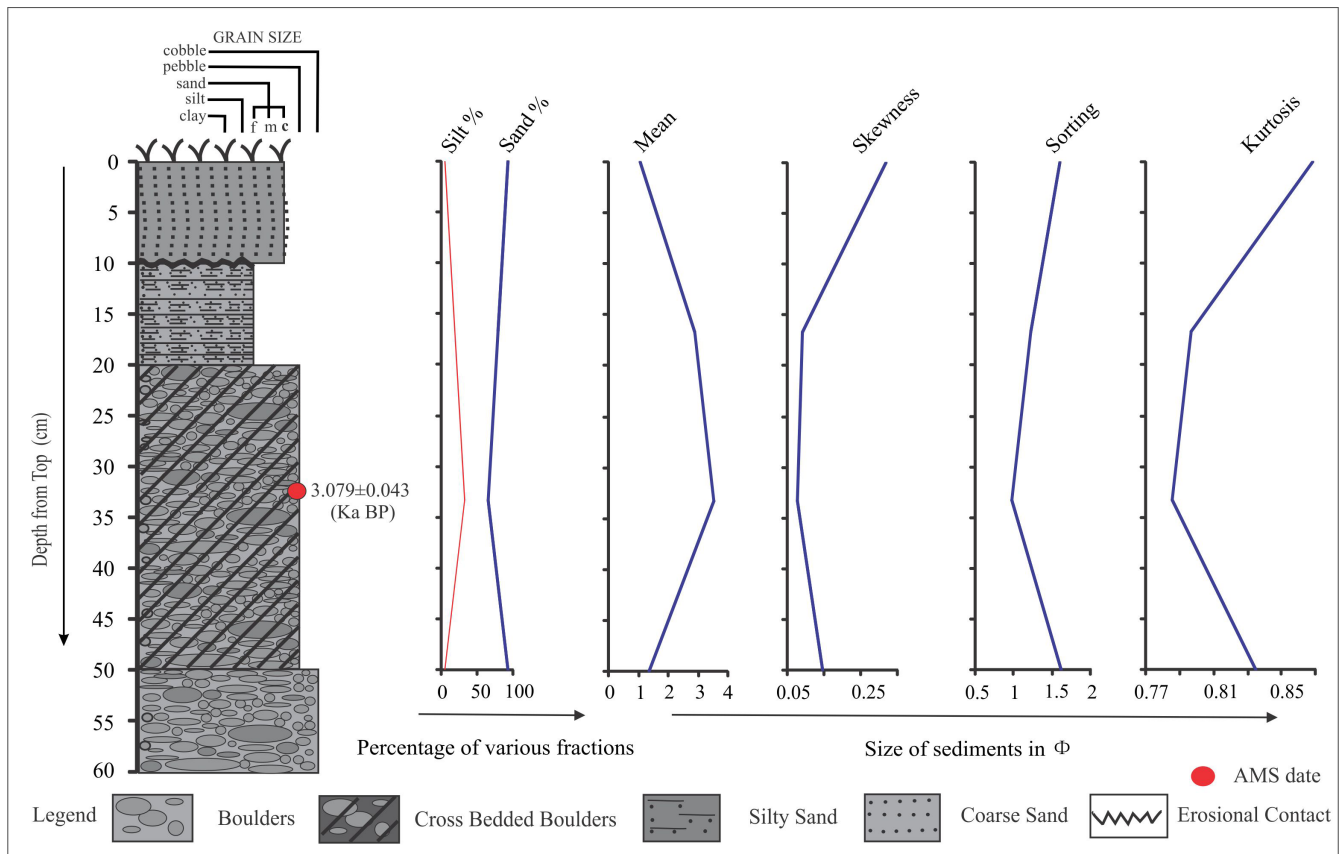
Fig. 11. Showing litholog and sediment grain parameters of outwash plain deposits.

The OWP lithology reflects the stratified deposits of sand and silt sediments with gravels (Fig. 10b). The deposition of coarse-grained sediments with boulders under high energy fluctuating conditions is attributed to glacio-fluvial activity. Similar litological parameters have been identified from other regions for OWP deposits (Singh and Ravindra, 2011a,b; Singh *et al.,* 2017; 2019; 2022).

Kame terrace deposits

The sediment grain analysis such as mean gain size (M_Z), inclusive graphic standard deviation (σ_1), skewness (Sk_1) and kurtosis (K_G) of the kame terraces are shown in Fig. 13 and Table 5. The mean size (M_Z) varies from - 0.008 Φ to 2.70 Φ and the average value is 1.36 Φ. The kame terraces sediments consist of medium sand to very fine silt. Inclusive graphic standard deviation (σ_1) is varying from 1.17 Φ to 1.76 Φ. The sediments are moderately well sorted to poorly sorted. It explains the low to moderate energy of the depositional environment for a long period with fluctuating energy conditions.

Inclusive graphic skewness (Sk_1) is varying from 0.09 Φ to 0.94 Φ which indicates that the sediments are positively to very positively skewed and the average value is 0.22 Φ explains that the finer sediments are in excess. The value of inclusive graphic kurtosis (K_G) is varying from 0.56 Φ to 0.88 Φ and the average value for kurtosis is 0.78 Φ i.e. the

Table 5. Grain size parameters of kame terrace deposits.

| Sample Number	M_Z (Φ)	σ_1 (Φ)	Sk_1 (Φ)	K_G (Φ)
GKA15 1	0.36	1.54	0.55	0.61
GKA15 2	0.04	1.18	0.74	0.62
GKA15 3	- 0.008	1.17	0.87	0.69
GKA15 4	0.35	1.54	0.57	0.62
GKA15 5	0.66	1.75	0.42	0.58
GKA15 6	0.70	1.76	0.39	0.57
GKA15 7	0.71	1.76	0.37	0.57
GKA15 8	0.66	1.71	0.38	0.56
GKA15 9	0.56	1.65	0.42	0.57
GKA15 10	0.53	1.64	0.43	0.58
GKA15 11	0.52	1.64	0.45	0.58
GKA15 12	0.55	1.66	0.43	0.58
GKA15 13	0.55	1.66	0.43	0.58
GKA15 14	0.61	1.69	0.41	0.57
GKA15 15	0.68	1.73	0.38	0.56
GKA15 16	0.72	1.76	0.37	0.57
GKA15 17	0.71	1.75	0.37	0.57
GKA15 18	0.71	1.76	0.37	0.57
GKA15 19	0.72	1.76	0.37	0.56
GKA15 20	0.72	1.76	0.37	0.56
GKA15 21	0.56	1.65	0.42	0.56
GKA15 22	0.56	1.65	0.43	0.56
GKA15 23	0.61	1.67	0.39	0.56
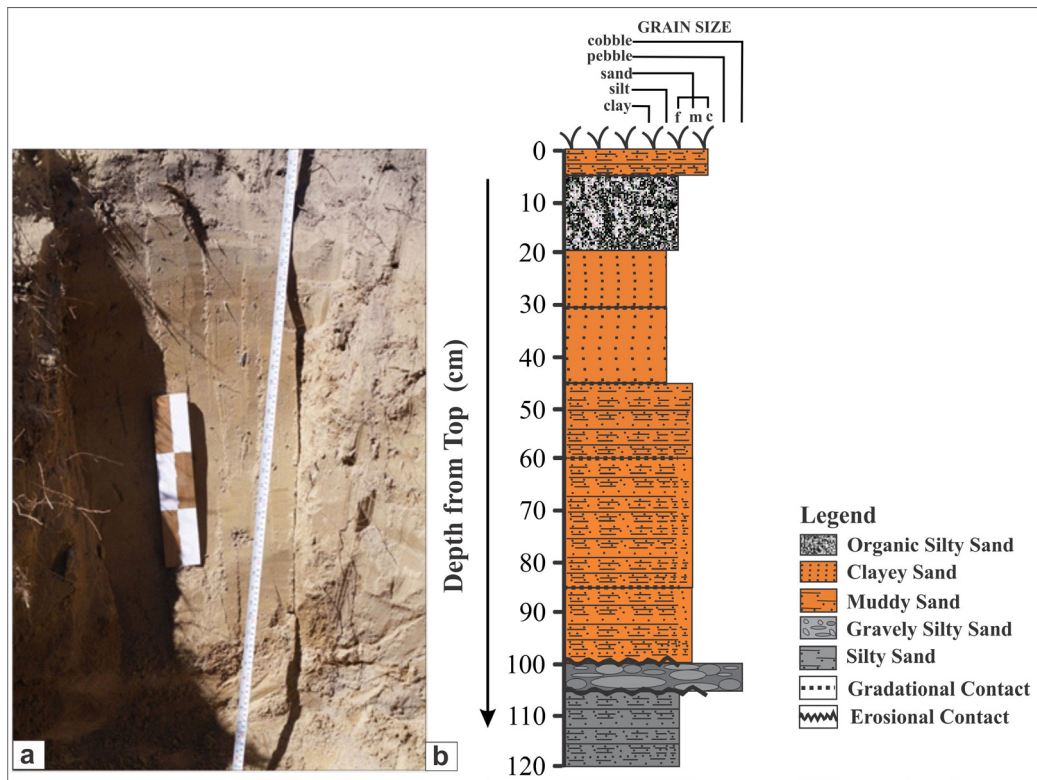
Fig. 12. (a) Photograph showing trench in kame terraces; (b) litholog of the trench (Singh *et al.*, 2019).

sediments are platykurtic to very platykurtic. It explains the predominance of finer sediments and better sorting of the tails.

The frequency distribution curves are shown in Fig. 14 a,b. It is showing the weight percentage of different sediment fractions. The absence of polymodal distribution indicates that the sediments may have been derived from a single source, as polymodal distribution is produced as a result of deposition from many different sources. It can be observed from these curves that the weight percentage of medium sand dominates followed by fine sand and very fine sand.

The KT deposits consist of gravel, sand, silt, and clay size (Fig. 12 a,b and Table 6) sediments in different proportions from bottom to top. The base is characterised by poorly-sorted gravely-sand deposited by glacial processes. The presence of clay from bottom to top varying in percentage from 25-55% (Fig. 13), explains the stagnant low-energy ponding condition. Thinly bedded parallel/horizontal laminations and organic matter are the most important features of such environment. Similar, deposits have been described from GGR (Singh *et al.*, 2019; Dubey *et al.*, 2022) and from other regions of the Himalaya (Bali *et al.*, 2017 a,b) and from the lacustrine deposits of the Ganga Plain also (Singh *et al.*, 2011; Trivedi *et al.*, 2011; Singh *et al.*, 2015; Saxena and Singh, 2017).

The KT deposits evolved by a combination of two depositional environments, the glacio-fluvial at the base and the lacustrine at the top. The KT exhibit the increased percentage of coarser sediments during more melting, more precipitation during the warm stages and intense ISM, and an increased percentage of the finer sediments during less melting, cold stages, and weak ISM.

Table 6. Weight percentage of various grain size fractions for kame terrace deposits.

Sample Number	V. C. Sand	C. Sand	M. Sand	F. Sand	V. F. Sand	Silt
GKA15 1	50.1	16.6	13.7	10.1	5.9	3.8
GKA15 2	57.3	18.8	12.7	6.6	2.8	1.7
GKA15 3	61.2	17.4	9.5	6.3	3.3	2.2
GKA15 4	50.4	16.7	13.5	9.7	5.8	3.9
GKA15 5	44.4	14.8	13.7	12.8	8.8	6.0
GKA15 6	43.5	14.5	14.0	12.8	9.2	6.1
GKA15 7	42.9	14.3	14.3	13.2	9.2	6.1
GKA15 8	43.7	14.6	14.5	13.2	8.7	5.3
GKA15 9	45.4	15.1	14.6	12.8	7.8	4.3
GKA15 10	45.9	15.3	14.9	12.5	7.3	4.2
GKA15 11	46.2	15.4	14.6	12.3	7.2	4.3
GKA15 12	45.7	15.2	14.5	12.4	7.6	4.5
GKA15 13	45.7	15.2	14.5	12.5	7.6	4.5
GKA15 14	44.7	14.9	14.3	12.8	8.3	5.0
GKA15 15	43.3	14.4	14.4	13.2	9.0	5.6
GKA15 16	42.9	14.3	14.3	13.2	9.2	6.1
GKA15 17	43.0	14.3	14.3	13.2	9.2	5.9
GKA15 18	43.0	14.3	14.3	13.1	9.2	6.0
GKA15 19	42.8	14.3	14.2	13.1	9.5	6.1
GKA15 20	42.8	14.3	14.2	13.2	9.5	6.0
GKA15 21	45.4	15.1	14.4	12.7	8.2	4.1
GKA15 22	45.5	15.1	14.4	12.8	8.1	4.0
GKA15 23	44.4	14.8	14.8	13.3	8.2	4.6

The sediment grain parameters have been used for the interpretation of sedimentary processes, reconstruction of climate change and monsoon variability (Eyles *et al.*, 1983; Kick, 1986; Kuhle, 1986, 1997; Richards *et al.*, 2000;
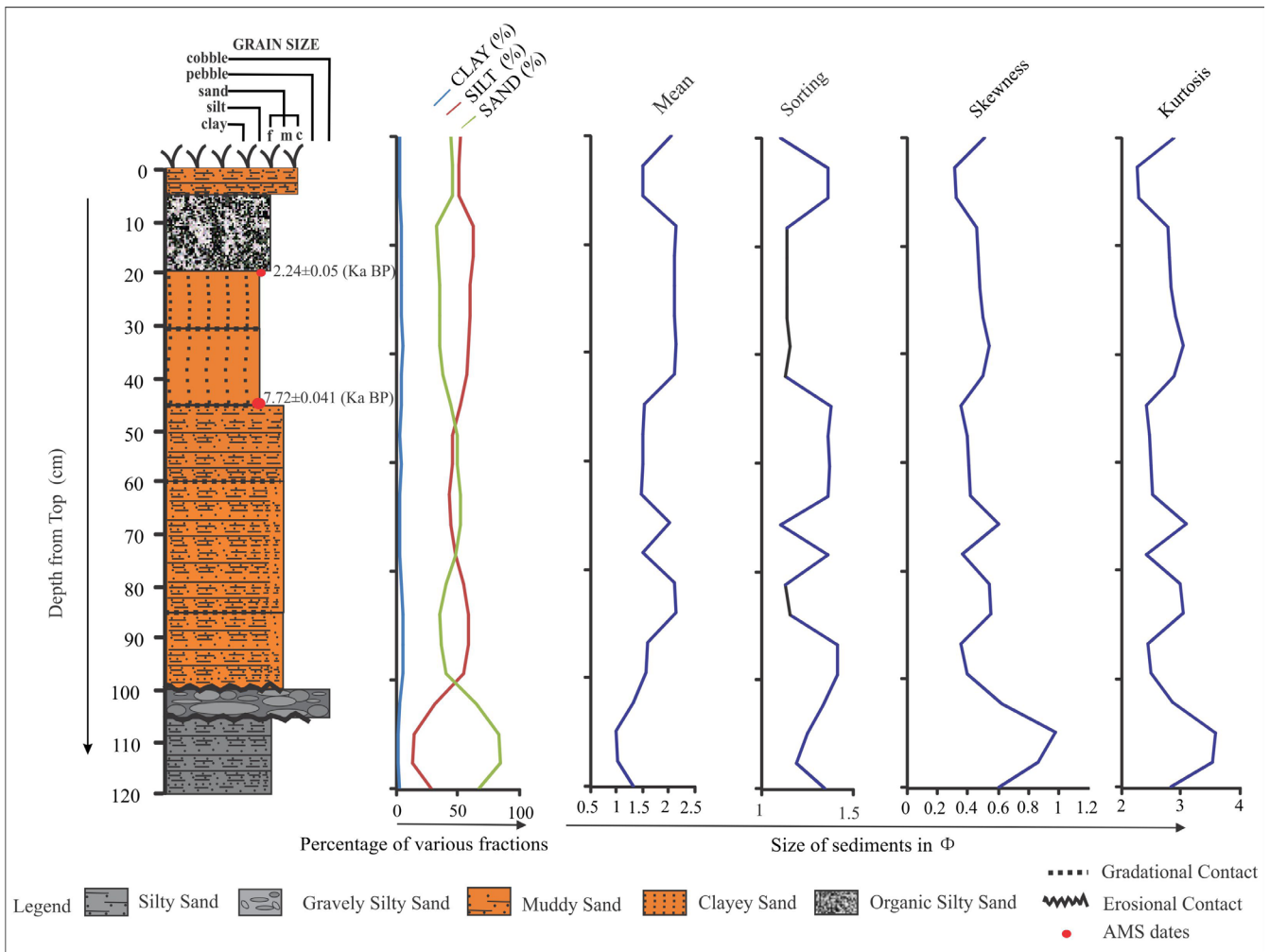
Fig. 13. Showing litholog and sediment grain parameters of kame terrace (Singh *et al.,* 2019).
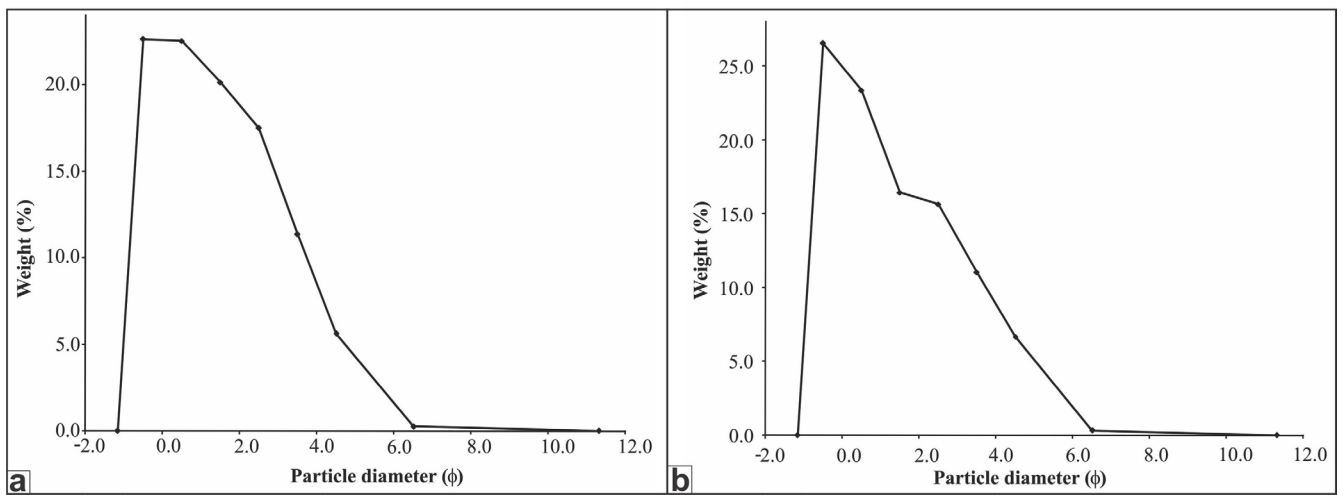

Fig. 14. (a) Frequency distribution curve for the sediments of outwash plain deposits; (b) Frequency distribution curve for the sediments of kame terrace deposits.
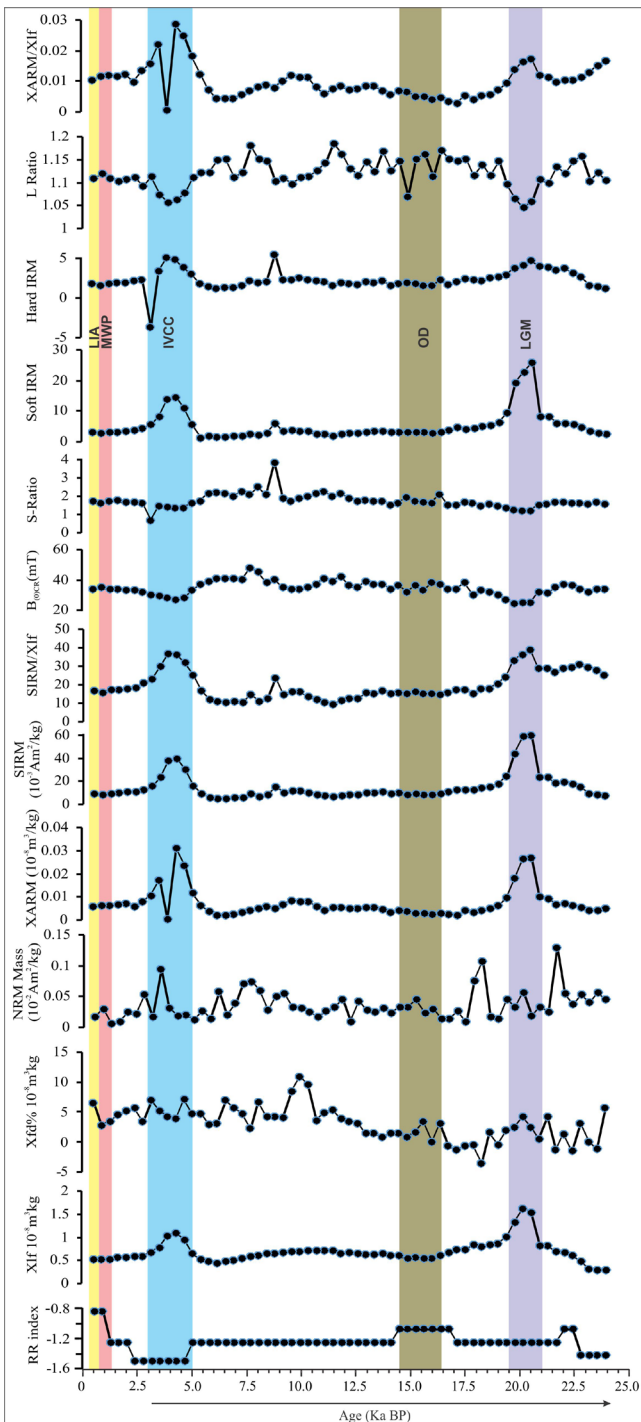
Fig. 15. Mineral magnetic parameters plotted against the calibrated ages for kame terrace deposits (Dubey *et al.,* 2022).

Mineral magnetism

The mineral magnetic applications to glacial rocesses is still under infancy and several case studies (e.g., Sangode and Bloemendal, 2004; Sangode et al 2007) are required to understand the process and application in relation to different types of glacial/glacio-fluvial deposits. We present one such case study from the kame terrace deposits to demonstrate the applicability of mineral magnetism in the glacial regimes.

Kame Terraces (KT)

One of the well exposed kame terraces was sampled from the GGR to examine the application of mineral magnetism (Dubey *et al.,* 2022). The most fundamental mineral magnetic parameter, the magnetic susceptibility in this kame terrace is controlled by detrital flux depicting the episodes of melt water influxes. The higher influx is reflected by lower magnetic susceptibility therefore it defines a proxy to retreating conditions experienced by the given depositional surface. Other mineral magnetic parameters further produce finer information on the reducing/ponding/ pedogenic conditions over the depositional surface at various times of emerging climatic episodes.
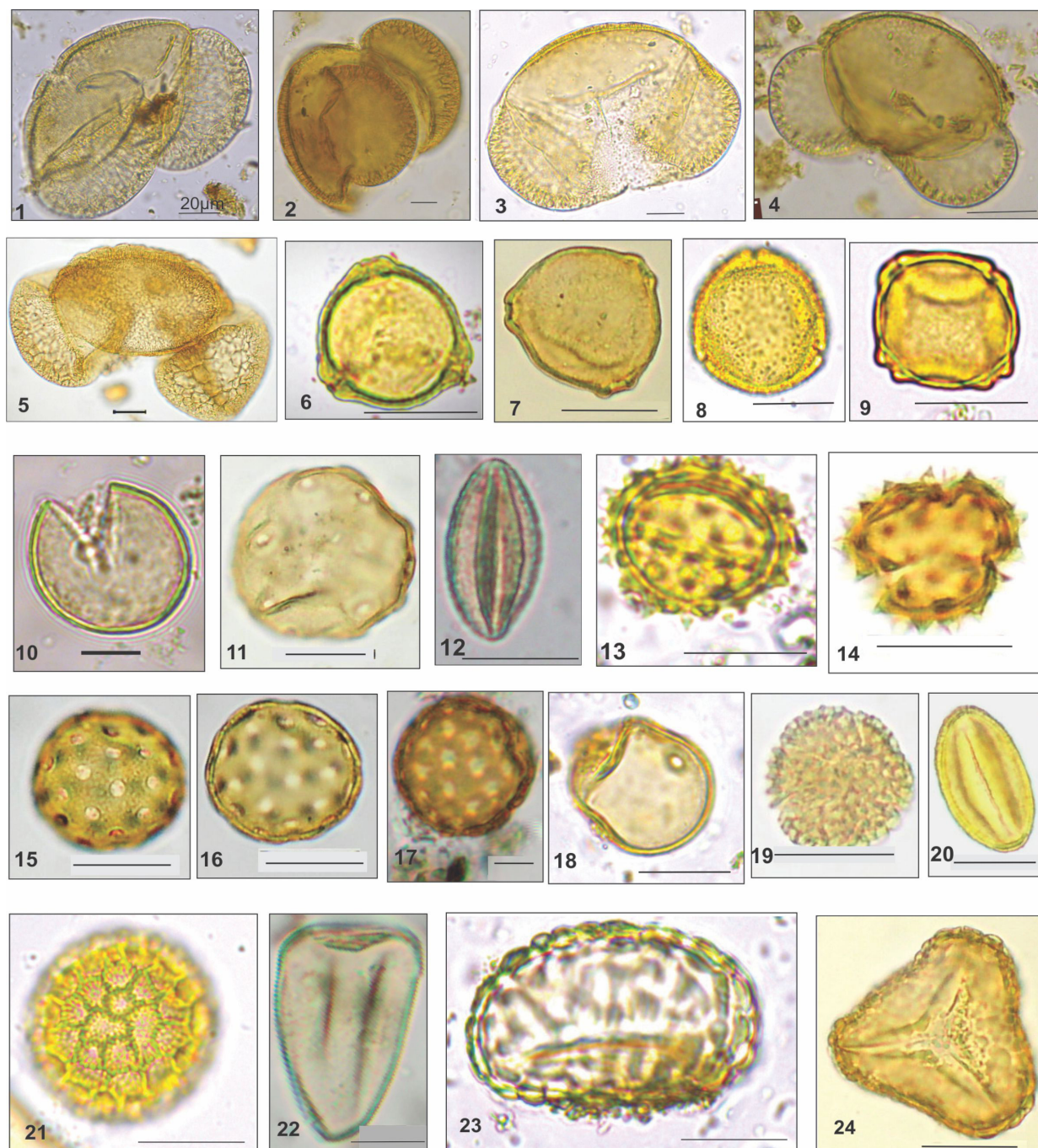
Overall the coarser fraction shows lower susceptibility depicting dia- and para magnetic contributions diluting the total susceptibilities. Similar mean and median values of susceptibility show low variability depicting negligible variation in the concentration of magnetic minerals. Higher Xfd% with maximum values (Fig. 15) indicated contribution from the SP ferrimagnets possibly from pedogenic sources in catchment.

The X_{ARM} depicts the concentration of SD Ferrimagnets indicating less oxygenated/reducing conditions. The S-Ratios indicates mixed mineralogy from ferrimagnetic to antiferromagnetic oxides with bias towards the latter in bulk form. The mean $Soft_{IRM}$ significantly higher than the Hard IRM depict the dominance of ferri over antiferromagnetic mineralogy.

The routine mineral magnetic parameters are therefore combined to produce elaborate information on the episodes of change in melt water production, well oxygenated to reducing and non- depositional conditions. This information is further readily combined with other proxies and age controls produced records of major climatic events, such as Last Glacial Maximum (LGM), Older Dryas (OD), Bølling-Allerød (BA), Younger Dryas (YD), Indus Valley Civilization Collapse (IVCC), Medieval Warm Period (MWP) and Little Ice Age (LIA). Similar approaches using the mineral magnetic approach can be made on the terrace profiles available in the glaciated valleys, the OWP sedimentation, moraines, glacial lakes etc.

The low SIRM, $Soft_{IRM}$ and X_{ARM} (Fig. 15) indicated low ferromagnetic concentration with low variability. The X_{lf} shows a significant positive correlation with X_{ARM}, SIRM, $Soft_{IRM}$ and $hard_{IRM}$. This indicates the strong ferrimagnetic bias of the X_{lf}. The NRM shows its bias towards X_{ARM} by displaying positive correlation. Overall the lowermost unit shows detrital (melt water) influx depicting warm episodes with well-oxygenated lacustrine conditions that ended with restricted events of cold climate. This is terminated again

Srivastava *et al.,* 2003; Singh and Singh, 2005; Juyal *et al.,* 2009, 2010; Singh *et al.,* 2009, 2010; Singh and Awasthi, 2011a,b; Dobhal *et al.*, 2013, 2021; Singh *et al.,* 1999; 2013, 2018, 2019; Singh, 2018). The sand deposition reflects the erosional environment, high intensity of monsoon rainfall and warm climatic conditions (Lee *et al.,* 2014). On the other hand, the clay deposition reflects the low precipitation (arid environment) and cold conditions.

Fig. 16. Palynomorphs recovered from the kame terrace sediments as: 1. and 2. Abies, 3. Picea, 4. Pinus, 5. Cedrus, 6. Betula, 7. Corylus, 8. Carpinus, 9. Alnus, 10. Juniperus, 11. Juglans, 12. Ephedra, 13 and 14. Asteraceae, 15 and 16. Chenopodiaceae. 17.Caryophyllaceae, 18. Poaceae, 20. Ranunculaceae, 21. Polygonumserrulatum, 22. Cyperaceae, 23. Fern monolete, 24. Fern trilete.

by melt water influx as marked by the detrital sediments at the top. Thus, the variations in mineral magnetic parameters in the studied profiles reflect the changes in depositional environment that are in turn governed by the climate change experienced in the Gangotri valley of the Garhwal Himalaya.

Palynology

In recent years, some palynological data have been generated from glaciated sites of Western Himalaya and it has been found that pollen-spores can be used as an important parameter to know the possible extent of the glaciers during Late Quaternary. The distribution of pollen-spores of the type vegetation with dating, is important to get the chronological history of various glacial stages. Palynological analyses of the kame terraces show the presence of pollen-spores (Fig. 16) of local terrestrial herbaceous as well as marshy taxa, along with the temperate tree taxa, transported from lower altitudes in good amount during Early Holocene.

GGR enjoyed a warm and moderately humid moist climate as deciphered by the presence of *Betula* dominant

alpine-scrub vegetation. The pollen signals are also indicated that during Early Holocene, i.e. around 9 Ka BP the site of kame terraces were free from glacial ice, and giving open ground for the growth of local herbaceous taxa (Ranhotra and Kar, 2011). This can be possible only if lateral levels of the Gangotri glacier were below the altitude of Kame terrace. This suggests that during Early Holocene, though the snout of the glacier would have been at a much lower altitude than the present day (4100 m amsl), the lateral levels of the Gangotri Glacier must have been below the altitude of pollen analysis (Ranhotra and Kar, 2011). Also, the glacier was retreating under warm–moist climate, which is evident by the presence of local marshy taxa and temperate tree taxa in good amount. The Late Holocene record of the GGR discussed through the pollen analysis of the Bhujbas OWP sedimentary profile (Kar *et al.*, 2002) indicate cool climate since 800 yrs BP till the time span coinciding with Little Ice Age (LIA), when the Gangotri glacier might have been stagnant.

The pollen analysis has revealed that during Early to Middle Holocene, the pollen frequency of tree-line forming taxa, viz. *Betula* and *Juniperus* (Kar *et al.,* 2002; Ranhotra and Kar, 2011) was higher than that during Late Holocene. This shows that during Early to Middle Holocene, the tree-line formed by *Betula* and *Juniperus* was as low as around the altitude of the study site (3100 m amsl) compared to the present-day level between 3800 and 3900 m amsl within the valley. Also, the fair number of conifers along with low pollen concentration of temperate, broadleaved taxa during Early to Middle Holocene indicates that conifer–broadleaved temperate forest was located further downstream than its present-day altitude and its pollen must have been transported by the wind to the study site. During Late Holocene, the decrease in pollen frequency of *Betula* and *Juniperus*, and increase in the pollen values of conifer–broadleaved temperate taxa indicate that these elements might have shifted to higher elevations with the retreat of the glacier under warm conditions.

In the last few years, palynological studies of some geomorphic features have been carried out from the Gangotri (Ranhotra *et al.,* 2001; Kar *et al.,* 2002; Ranhotra and Bhattacharyya , 2004), Baspa (Bhattacharyya *et al.,* 2021; Chakraborty *et al.,* 2006; Ranhotra and Bhattacharyya, 2010) and Chaurabari (Kar, 2008) glaciated valleys of the Western Himalayan region. Some palynological data have been generated from a few glaciated sites of Western Himalaya and it has been found that other than palaeoclimatic reconstruction, pollen-spores can be used as an important parameter to know the possible extent of the glaciers during Late Quaternary. Glacier dynamics plays an important role in carving and consequent modification of the various geomorphic features, which are the characteristic of various stages of glacial fluctuations. Because the distribution of pollen-spores of the type vegetation is ubiquitous, collection of subsurface sediments from the depositional geomorphic features, for palynological study as well as dating, is important to get the chronological history of various glacial stages.

Carbon deposition

Total organic carbon (TOC) and its stable isotopic

measurements were carried out in the glacial stratified deposits in the Kame terrace. In addition to TOC, refractory portion of carbon i.e. soot carbon or Black carbon (BC) and its stable isotopes were also measured. BC dispersion and its eventual over Indian glaciers is highly debated due to its capability in absorbing radiation and then re-radiate it after its removal from the atmosphere. It may provide an additional source of heating snow cover and promote glacier melting via entirely different pathways unlike the greenhouse effect exerted gases like CO_2, CH_4 and N_2O. BC containing glaciers may have different albedos. BC has very long residence time unlike organic carbon and other greenhouse gases. Data availability for BC and its stable isotope $\delta^{13}C_{BC}$ is highly sparse globally. Exact role of BC in glacier melting is not understood till today. In this study, we generated few data for BC and its stable isotopes to promote its usage in future studies.

$\delta^{13}C_{TC}$ and $\delta^{13}C_{BC}$ values increase in depth of trench. Overall, $\delta^{13}C_{TC}$ varies in range from - 22.8‰ to -24.6‰ and $\delta^{13}C_{BC}$ varies from -25.2‰ to -26.0‰ (Table 7). Terrestrial C_3 plants typically display $\delta^{13}C$ values between −24 to −34‰, averaging ~ −27±2‰ (Faure, 1998; Kohn, 2010). In-situ produced organics such as algae and lichens normally have $\delta^{13}C$ values between −12 to −23‰ (Lange *et al*., 1988; Lee *et al*., 2009). Terrestrial C_3 vegetation dominated $\delta^{13}C$ values do have a rather exploitable relationship with mean annual precipitation of the region. Higher $\delta^{13}C$ values generally > -25.5‰ represent terrestrial environments with lesser MAP (< 500 mm/yr), however, for wetter environments sensitivity of $\delta^{13}C$ values against MAP weakens. Grasses, on the hand, generally found in follow C_4 pathway of metabolism that involves relatively lesser fractionation compared to those following C_3 pathway (generally woody plants) and hence display enriched $\delta^{13}C$ values averaging about −12.5‰ (Faure, 1998).

Table 7. Shows the variation in TC (wt.%) and BC (wt.%) with increase in the depth of kame terrace deposits.

Depth (cm)	$\delta^{13}C_{TC}$	TC (wt.%)	$\delta^{13}C_{BC}$	BC (wt.%)
0	24.6	0.91	-25.2	0.03
5	23.9	0.9	-25.5	0.08
10	23.9	2.5		
15	23.4	1.36	-24.2	0.08
20	23.1	1.03	-24.4	0.08
25	22.9	1		
30	23.9	0.26	-26	0.09
35	23.1	0.73	-25.8	0.08
40	23.1	0.77	25.4	0.08
45	23.1	0.83		
50	23.4	0.54		
55	23.3	0.45		
60	23.5	0.38		
70	23.8	0.27		
75	22.8	0.88		
80	24.1	0.26		
85	24	0.34		
90	23.8	0.46		
95	23.7	0.5		
	-23.5	0.75	-25.2	0.07
STD Deviation	0.5	0.52	0.7	0.02

TC (wt.%) varied in the range from 0.26 to 2.5 %, with an average value of~0.75±0.52 % (n=19). Whereas, BC contents varied from 0.03 to 0.09% with an average of ~0.07±0.02 (n=7). $\delta^{13}C_{TC}$ values varied in the range from -22.8 to -24.6‰ with average value of -23.5 ±0.5‰ (n=19) and $\delta^{13}C_{BC}$ values varied in a narrow range from −25.2 to −26.0‰ with an average value of -25.2±0.7‰ (n=7). Average $\delta^{13}C_{TC}$ values the trench (−23.5‰) indicate that the trench possibly has organic material of both C_3 and C_4 type i.e. mixed type of vegetation. The average BC content in the trench II is ~0.07% which is roughly ~10% of the total carbon content. $\delta^{13}C_{BC}$ of trench II (−25.2‰) closely resembles $\delta^{13}C$ values (~ −26‰) of atmospheric aerosols from polluted valley region of Indo-Gangetic plains (Sawlani *et al.*, 2019).

Kame terrace trench is characterized by both C_3-C_4 i.e. mixed type (Table 7) of vegetation. Vegetation like maize but also in millet, sorghum, sugarcane and crabgrass& grasses in hot arid climatic conditions follow a C_3 photosynthesis pathway while grasses in temperate climates (barley, rice, wheat, rye and oats, sunflower, potato, tomatoes, peanuts, cotton& most trees and their nuts/fruits, roses and Kentucky blue grass) follow a C_3 photosynthetic pathway. So this trench should be characterized by both the types of vegetation. The carbon isotopic analysis shows that the region is characterized by both C_3-C_4 i.e. mixed type of vegetation. The average value in the weight % of soot proportion (Black carbon content, BC hence forth) is 0.07% and typical $\delta^{13}C_{BC}$ is −25.2‰ which is close to atmospheric aerosols containing vehicular emissions mainly during the common traffic (~ −26‰).

Processes of landscape modification

Glacial is the primary process dominant during glacial stage whereas fluvial, mass movement, lacustrine, and flash floods (LLOF and GLOF) known as secondary/non-glacial/paraglacial came into existence during interglacial stages (Singh, 2004) in a glaciated terrain. The paraglacial processes are more complex (Ballantyne, 2002) and originate due to recession (Singh, 2004) over a wide range of timescales. The paraglacial processes affect and modify the pre-existing landforms due to recycling of the sediments (Evans *et al.*, 1995; Singh and Mishra, 2002a).

We have reported that the tributary glaciers (Singh and Mishra, 2002a), snow-melt ephemeral streams (Singh, 2013a), landslide lake outburst flooding (LLOF) (Singh and Mishra, 2002a; Singh, 2013b, 2014) and glacial lake outburst flooding (GLOF) (Singh, 2013b, 2014) are the important processes, which affect, modify, and often washed out the earlier glacier signatures, making it difficult to identify the landforms, and thus provide the diversified data for retreat and climatic events.

Tributary Glaciers and Landslide Lake Outburst Flooding (LLOF)

In Bhujbas area, on 6th June 2000, heavy rains (80 mm) transported huge amount of sediments from the left bank tributary glaciers and deposited enormous amount of sediments into the valley. The transported sediments consisting of boulders, pebbles, cobbles, sand and silt dammed the Bhagirathi river and formed a short-lived extensive ephemeral lake. Bursting of this lake created the flash floods near Bhujbas. At places 1-1.5m thick sediments were deposited (Fig. 9b). The tributary glaciers caused the LLOF, which recycle and redistribute the sediments thus affecting the existing landscape and play an important role in the sedimentation of the Bhagirathi valley (Singh and Mishra; 2001, 2002a, 2002b).

Snow Melt Ephemeral Stream

GGR is completely covered with snow during the winter season. Remote sensing satellite data indicate that the snowfall during winter season (accumulation period) is about 10 times higher than the permanent snow and ice in the Himalaya (Tangri, 2002). It has been observed that building up of snow cover starts from October to December, develops during January to March and starts ablating from April onwards, reaching a minimum in September (Singh, 2013a). The melting of snow due to increase in temperature and change of season generate the ephemeral streams. The snow-melt ephemeral streams on the top surface of a glacier, better known as supraglacial streams, erode the finer sediments from the pre-existing landforms and thus modify the pre-existing landforms (Singh, 2013a). As a result, the lithology changes from the matrix-supported boulders to the clast-supported boulders.

Glacial Lake Outburst Flooding (GLOF)

The accumulation zone of the Gangotri glacier is characterized by the abundance of supraglacial lakes. The mass movements, mainly the landslides and debris flow may transport huge amount of sediments and dammed the lakes, which are overfilled by prolonged heavy rains. The increasing water pressure causes bursting of these lakes, which creates the flash floods. In the Kedarnath area, bursting of Gandhi Sarovar and the short lived ephemeral lakes, caused GLOF and LLOF in the area (Singh, 2013b, 2014). The differential erosion, redistribution and deposition of huge amount of poorly sorted sediments in the entire Kedarnath region modified the pre-existing glacial landforms and landscape.

Mass Movement

Satellite images (Fig. 17a,b) and field evidences (Fig. 18 a,b,c and d) indicate that the lower part of the Gangotri glacier experienced intensive mass movement in 2017. This mass movement transported and deposited the enormous sediments from the upper reaches to the lower area of the glacier, which breached the continuity of the left moraine (Fig. 18c). This deposited material shifted the Bhagirathi river between 2 m to 175 m (Fig. 18a and b). About 1560 m length of the river and around 360700.00 m² area of the valley was covered by the sediments. A dammed lake adjacent to the snout of the Gangotri glacier (Gaumukh) was formed (Fig. 18d). The detailed analysis of the IMD data (A.K. Singh *et al.*, 2020) with Google Earth images suggested that intense precipitation, large debris flow, slope failure, collapse of
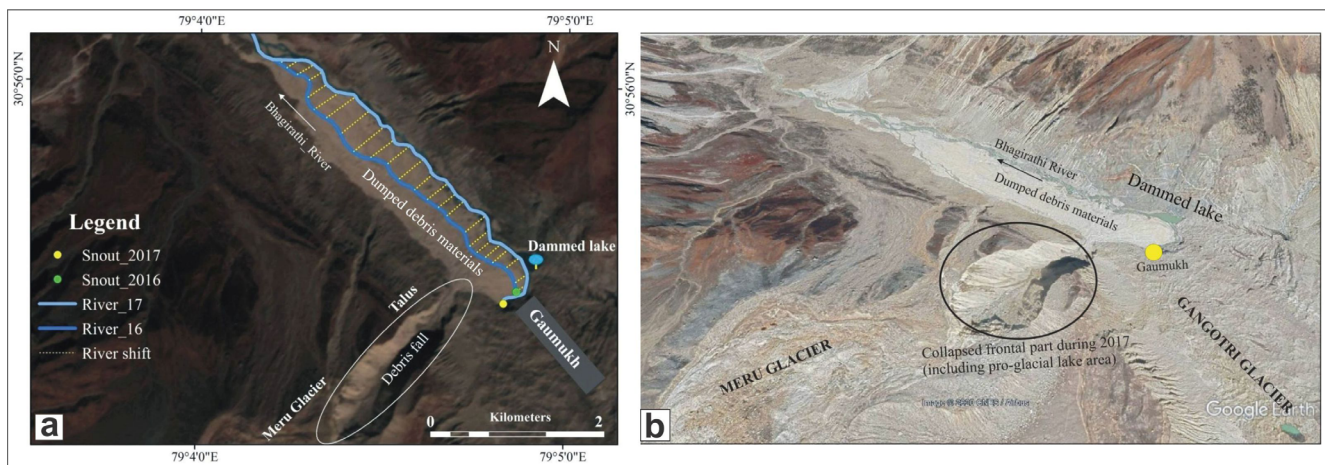
Fig. 17. (a) Event of intense mass movement during 2017 at Bhagirathi valley; (b) Google Earth image (07/10/2017) showing collapsed frontal part of the Meru glacier and dumped debris material within the Bhagirathi valley (A.K. Singh *et al.,* 2020).

Table 8. Geochronology of GGR based on AMS ages for outwash plain and kame terrace deposits.

S. No.	Geomorphic feature	Nature	Trench No.	Depth (cm)	Location of the Trench (Latitude; Longitude and Elevation)	Calibrated AMS Ages (Ka BP)	Time (Ka BP)
1	Outwash Plains	Glacial stratified	I	33	N 30°56'59.2"; E 79°03'3.6" and elevation: 3796 m	3.079	~4.0
2	Kame terraces	Glacial stratified	II	20	N 30°57'00"; E 79°03'28" and elevation: 3945 m	2.246	~25.0
3				45		7.72	
4				10	N 30°57'04"; E 79° 03'28" and elevation: 3945 m	0.084	
5	Kame terraces	Glacial stratified	III	35		3.557	~14.0
6				100		12.631	
7	Kame terraces	Glacial stratified	IV	37	N 30°56'54.7"; E 79°03'35" and elevation: 3990 m	5.408	~25.0

frontal part of the Gangotri glacier were responsible factors for this mass movement.

The controversy for the rate of retreat, extent of glacier during LGM, geochronology and palaeoclimate (Zheng and Rutter, 1998) exist because of the problems in the identification of landforms (Benn and Owen, 1998, 2002), due to its modification by the non-glacial processes which evolve during deglaciation (Singh and Mishra, 2002a; Singh and Mishra, 2002b; Singh, 2013a; Singh, 2013b; Singh, 2014). It creates confusion in the identification of diamictons (Owen *et al.,* 1998, 2002, 2008). It is believed that during deglaciation, sediment recycling is high due to unstable sediments and poorly developed vegetation cover (Ryder, 1971; (Hewitt, 1993; Benn and Evans, 1998), which also affect the landforms.

Geochronology and major climatic events

Seven Organic rich sediment samples were collected for ^{14}C AMS dates from the stratified deposits of KT, and OWP. Table 8 shows the various geochronological dates from GGR, from trench I at a depth of about 33 cm (3.079 Ka BP), trench II at 20 cm (2.246 Ka BP) and 45 cm (7.72 Ka BP) depths (Fig. 13), trench III at 10 cm (0.084 Ka BP), 35 cm (3.557 Ka BP) and 100 cm (12.631 Ka BP) depths, and trench IV at a depth of about 37 cm (5.408±0.056 Ka BP).

The geochronology of various sections of the glacial stratified deposits of KT provide the climate change of last 25 Ka BP with major warm and cold events (Fig. 19) such as Last Glacial Maximum (LGM) 21-19.5 Ka BP, Older Dryas (OD) 16.5-14.5 Ka BP, Bølling-Allerød (BA) 14.5-13.5 Ka BP, Younger Dryas (YD) 13.5-12 Ka BP, Indus Valley Civilization Collapse (IVCC) 5.0-3.0 Ka BP, Medieval Warm Period (MWP) 1.25-0.7 Ka BP and Little Ice Age (LIA) 0.7-0.2 Ka BP. The IVCC, MWP and LIA events are also confirmed with OWP deposits (~ 4 Ka BP).

The glaciations in GGR between 63 to 11 Ka BP (Barnard *et al*., 2004) is comparable to present study having three major glaciation stages in trench IV between 25-10 Ka BP. The intense ISM (trench II and III) around 22.6 to 20.5 Ka BP and 20.5 to 18 Ka BP and weak ISM corresponding to Younger Dryas around 15.7 to 11.5 Ka BP are similar to the events of Bharatpur, Upper Lahaul Valley, NW Himalaya (Bohra *et al*., 2017). The present study explains six glaciation events after LGM around 14.5, 13.1, 10.1, 8.6, 7.5, 2.2 Ka BP, which are comparable to the glacial stages of Kedarnath region (Mehta *et al*., 2012).

The OD and YD events are marked as weak precipitation events (Fig. 19), whereas the Allerød interstadial event as wet periods. The multi-proxy's analysis in existing literature (Kotlia *et al.,* 2010) provides the LGM, OD, YD events (Rawat *et al.,* 2015; Kotlia *et al.,* 2016; Dubey *et al*., 2022)
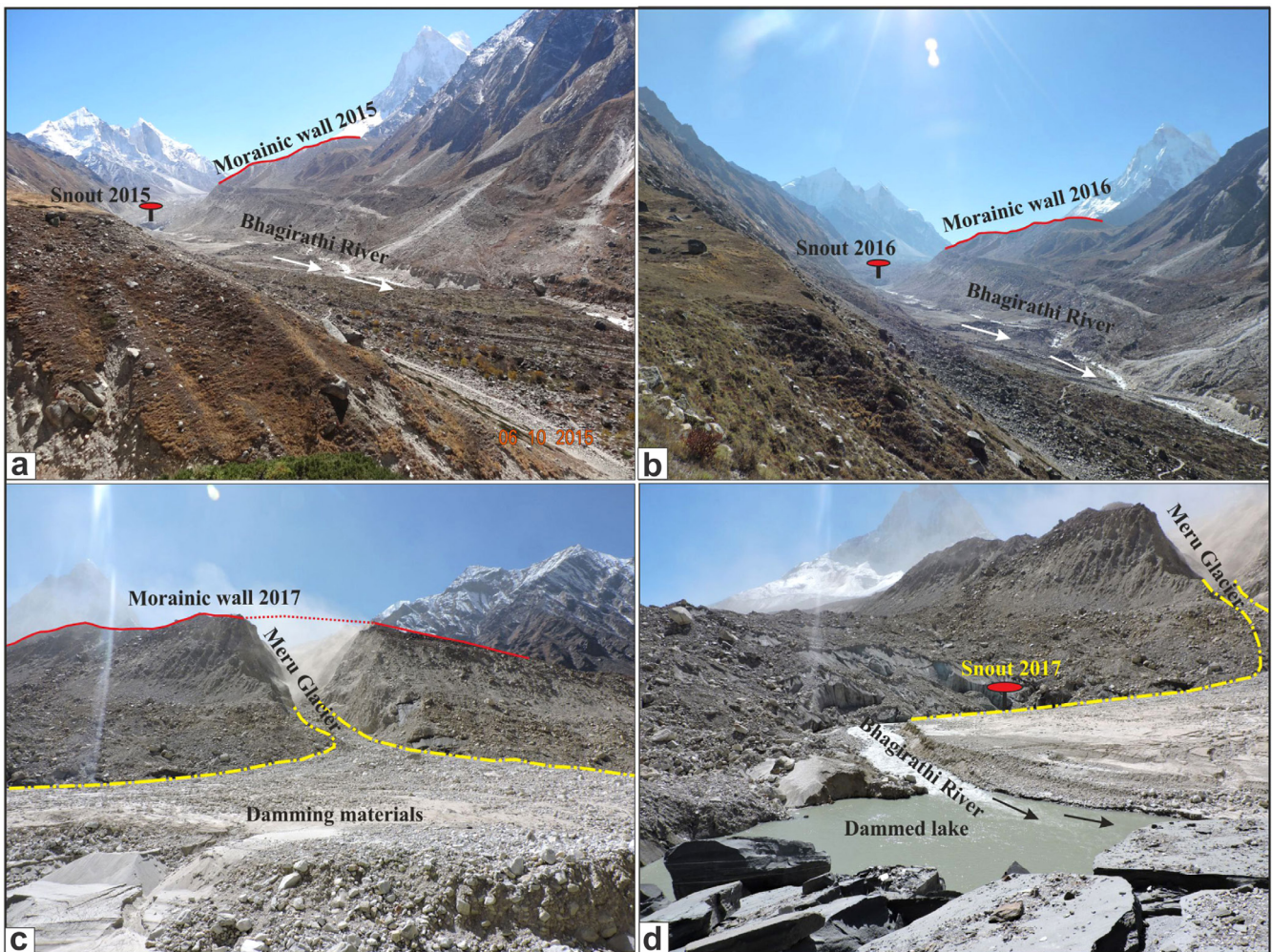
Fig. 18. (a) Field photographs showing the snout position of Gangotri glacier and continuity of left morainic wall in 2015; (b) the snout position of Gangotri glacier and continuity of left morainic wall in 2016; (c) breached morainic wall and debris flow during 2017; (d) dammed lake adjacent to the snout of Gangotri glacier (A.K. Singh *et al.,* 2020).

similar to the present study. The intense ISM around 18±2, 15±1, 8±1 Ka BP in the Alaknanda Valley (Juyal *et al.,* 2010) are also comparable to the climate events of the present study. The BA is well marked as warm and wet phase from approximately 14.5 to 12.5 Ka BP in Northern Hemisphere (Alley *et al.,* 1993). In our records, the Allerød interstadial ranges between 14.5-13.5 Ka BP.

The present study reveals a precipitation failure from 5.0- 3.0 Ka BP (Fig. 19), which can be linked with the decline of the IVCC from 5 Ka BP onwards which was completely collapsed between 3.5 to 3 Ka BP (Leipe *et al.,* 2014). Our records show peak aridity between 3.5 Ka BP to 3.1 Ka BP, which is similar to a distinct arid event in South Asia (Madella and Fuller, 2006; MacDonald, 2011). The alpine peat record from Central Indian Himalaya indicates an arid event between 4 to 3.5 Ka BP within the age uncertainties (Phadtare, 2000), which are close to our results. From ~2.2 Ka BP has been reported beginning of neoglacial stage and weak ISM resulting to ponding conditions (Bali *et al.,* 2017a,b), which is well correlated with present analysis.

In our records, the MWP ranges from 1.2- 0.6 Ka BP (750 to 1350 AD) on the basis of grain size parameter. The MWP duration is still debated for not being synchronous all over the globe (Bradley, 1992; Bradley and Jones, 1993). The Himalayan cave records (Sanwal *et al.,* 2013) show a little variation towards warm and described MWP as a regional event rather than a global event (Yang *et al.,* 2003; Singh *et al.,* 2019).

The OWP deposits show the LIA and post-LIA event between 0.6-0.3 Ka BP (1350-1650 AD) and 0.3-0.09 Ka BP (1650-1860 AD) respectively. In addition, the higher percentage of clay in both KT trenches (II and III) around 0.65–0.2 Ka BP (1300-1750 AD) and higher percentage of silt and low clay content around 1.15–0.55 Ka BP (800–1400 AD) validates the Little Ice Age (LIA) and Medieval Warm Period (MWP) respectively. Three stages of moraines are present near Bhujbas on the right bank, representing minor episodes of glacier advances (Singh *et al.,* 2017, 2019; Sharma and Owen, 1996) and probably represent the extent of the Little Ice Age (Srivastava, 2012).

Glacial stratigraphy

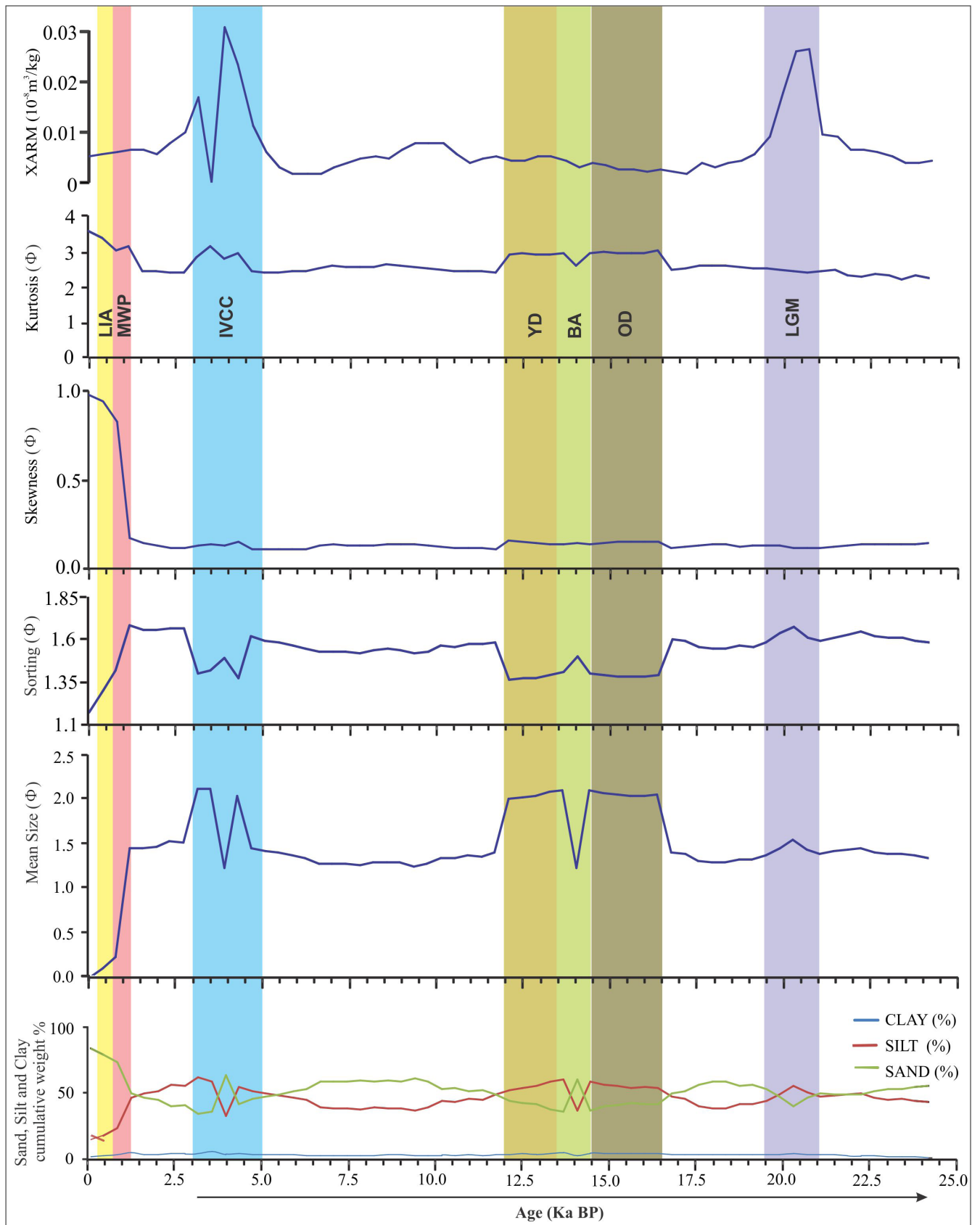The oldest age from the GGR is 63 Ka BP (Table 9) (Sharma and Owen, 1996), it indicates the maximum extent

Fig. 19. Correlation of sediment grain parameters of kame terrace deposits with major climatic events (Dubey *et al.,* 2022).

Table 9. Glacial stratigraphy of the GGR and the sequence of events of the various geomorphic surfaces.

S. No.	Landform	Nature	Age	Lithology
9	New Outwash Plain	Glacial stratified	1.82- 1.0 Ka BP (Barnard *et al.,* 2004)	35% boulders of varying sizes, poorly sorted, 30-40% matrix
8	New Lateral Moraine	Glacial unstratified	1.0- 0.35 Ka BP (Barnard *et al.,* 2004)	50% boulders of varying sizes, poorly sorted, 20-30% matrix
7	Debris Cone	Paraglacial unstratified	5.2- 1.8 Ka BP (Barnard *et al.,* 2004)	40-60% boulders Massive, unstratified, unconsolidated, moderately sorted
6	Old Outwash Plain	Glacial stratified	5.13±1.54- 3.3 Ka BP (Sharma and Owen, 1996) (Present Study)	55% boulders of varying sizes, very coarse to fine grained, layers of sand, silt, and clay
5	Old Lateral Moraine	Glacial unstratified	17.56±4.11- 4.84±1.21 Ka BP (Sharma and Owen, 1996)	50% boulders of varying sizes, poorly sorted, 30-40% matrix
4	Kame Terraces	Glacial stratified	25.0 - 0.3 Ka BP (Singh *et al.,* 2019; Dubey et al., 2022)	80-90% sand and silt, 10% clay, well sorted
3	Oldest Outwash Plain	Glacial stratified	~ 60 Ka BP	80% boulders and 20% matrix
2	Oldest Lateral Moraine	Glacial unstratified	~ 60 Ka BP	60% boulders of varying sizes, poorly sorted, 30-40% matrix
1	Terminal Moraine	Glacial unstratified	62.89±8.58 Ka BP (Sharma and Owen, 1996)	60-70% boulders of varying sizes, poorly sorted, matrix supported

of the glacier during the Pleistocene Ice Age (Fig. 20) and the oldest landforms to be evolved at that time was terminal moraine (~ 63 Ka BP). This glacial stage also evolved the associated oldest LM (~ 60 Ka BP) and oldest OWP (~ 60 Ka BP) when the glacier was stagnant for long duration. The signatures of oldest LM and OWP deposits might have washed out by the paraglacial process. The wide gap between the valley wall and first stage of the LM were filled by melt water, which evolved the lacustrine deposits above glacial deposits known as kame terraces (~ 25 Ka BP) (Singh *et al.,* 2019; Dubey *et al.,* 2022). After the evolution of old and new LM (1.0-0.35 Ka BP) and OWP (1.82-1.0 Ka BP) at different time span, the glacial retreat provided the accommodation space, where debris cones were formed during Late Holocene period (5.2- 1.8 Ka BP). On the basis of all available chronology from various geomorphic surfaces and field data the glacial stratigraphy has been established for the first time (Table 9, Fig. 20).

The Bhagirathi Glacial Stage is characterised by an extensive glaciation, when glaciers advanced and coalesced with the main Bhagirathi valley glacier (Sharma and Owen, 1996; Barnard *et al.,* 2004) up to Jhala (63 Ka BP). The LM of the Bhagirathi Glacial Stage can be traced up to Jhala (63 Ka BP) (Table 9). Thus, the date of ~ 63 ka BP at Jhala may represent the age of the maximum ice extent, while the dates of 17.5 ± 4.1 Ka BP (Jangla) and 5.1±1.5 Ka BP (at Bhujbas) suggests that these moraines date from a period of retreat during late Pleistocene and early Holocene times. Derbyshire *et al.* (1984) provide ages for the Borit Jheel Glaciation in the Hunza valley, northern Pakistan, of 47 ± 23 Ka BP to 65 ±33 Ka BP. Corresponding to the RM, there should be old OWP and old LM which might be washed out by the paraglacial processes. This is the reason that it is difficult to establish the extent of the glacier during LGM in the Himalaya in general and GGR in particular.

The recent studies suggest that KT (Singh *et al.,* 2019; Dubey *et al.,* 2022) were formed around 25 Ka BP, under low energy stagnant water conditions (lacustrine conditions). The pollen analysis supports the existence of KT between 9.0 Ka BP to 1.0 Ka BP. The Shivling Glacial Advance must have occurred after 5 Ka BP i.e. after the Bhagirathi Glacial Stage

moraines had formed near Bhujbas. During the Bhujbas Glacial Advance glaciers reached positions between 1 and 2.2 km beyond the recent location of snouts (Sharma and Owen, 1996; Barnard *et al.,* 2004). This advance occurred around 0.2 Ka BP to 0.3 Ka BP (Hodgson, 1822; Griesbach, 1891; Auden, 1937; Vohra, 1988; Sharma and Owen, 1996) in accordance with the Little Ice Age as found elsewhere in the Himalayan region (Derbyshire *et al.,* 1984; Fort, 1987; Barnard *et al.,* 2004) and in other parts of the world (Groves, 1988).

At the end of this glacial advance (Shivling Advance, ~5 Ka BP), the region near Gangotri village, including the mouth of the Kedar and Rudugaira valley, was the site of intense paraglacial process (Sharma and Owen, 1996; Barnard *et al.,* 2004). Abundant glacial sediment available upon the termination of the Shivling Advance were resedimented to form paraglacial debris flow fans.

CONCLUSIONS

The Gangotri glacier, one of the longest valley glaciers of the Garhwal Himalaya, located in the Uttarkashi district although retreating, the rate of retreat is decreasing (10-15 m/y between 2015-2021). The decreasing rate of retreat is contrary to the anthropogenically induced global warming. Tree-ring study with precise dating control revealed the accurate location of the Gangotri glacier terminus ~1.853 km down from its recent position (i.e. July, 2017) in the late 16th century (1571 C.E.). However, earlier geochronological dates based studies indicated the glacier terminus around 3.7 km down during ~200-300 yrs B.P from its position in the year 1992.

The study explains that GGR exhibits glacial as well as non-glacial landforms. The glacial landforms are both stratified and unstratified in nature. The unstratified glacial deposits are Lateral Moraines, Terminal/Recessional Moraines, whereas stratified deposits are Outwash Plains and
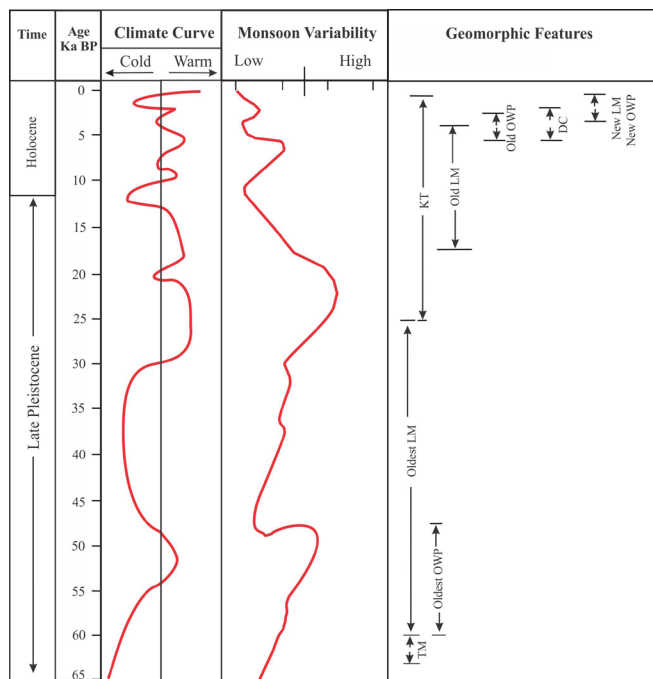
Fig. 20. Showing time frame for the evolution of geomorphic features in the GGR and also the Pleistocene-Holocene climatic and monsoon variability (SW Indian Monsoon and Westerlies) (TM: Terminal Moraines, LM: Lateral Moraines, OWP: Outwash Plains, DC: Debris Cones).

Kame Terraces. The non-glacial landforms are Debris Cones, Pillar Structures and Flash Flood Deposits. A geomorphic map was prepared and a model for the geomorphic evolution of the GGR was proposed.

The sediment grain parameters of OWP deposits show that mean grain size (M_Z) varies from 0.25 Φ to 3.52 Φ; and the standard deviation (σ_1) varies from 0.98 Φ to 1.68 Φ. The OWP deposits consist of medium sand sediments which are poorly sorted. The inclusive graphic skewness (Sk_1) value ranges from 0.07 Φ to 0.42 Φ i.e. from symmetrically skewed to very positively skewed, explaining excess of the finer sediments. Graphic kurtosis (K_G) ranges between 0.78 Φ to 1.06 Φ i.e. from platykurtic to mesokurtic, indicating predominance of finer sediments. The analysis explains that OWP deposits at Bhujbas were evolved by glacio-fluvial environment under fluctuating energy conditions.

The mean grain size of the KT deposits (M_Z) varies from - 0.008 Φ to 2.70 Φ and the inclusive graphic standard deviation (σ_1) varies from 1.17 Φ to 1.76 Φ. The kame terrace sediments consist of medium sand to very fine silt, which are poorly sorted. Inclusive graphic skewness (Sk_1) varying from 0.09 Φ to 0.94 Φ indicates that the sediments are positively to very positively skewed, which explains excess of finer sediments. The value of inclusive graphic kurtosis (K_G) is varying from 0.56 Φ to 0.88 Φ and the average value for kurtosis is 0.78 Φ i.e. the sediments are platykurtic to mesokurtic indicating the predominance of finer sediments and better sorting of the tails. The sediment grain analysis explains low to moderate energy of the depositional environment for a long period with fluctuating energy conditions. The lithology and granulometric analysis explain

that the sediments of the kame terraces are consolidated to semi consolidated, stratified, very coarse to fine-grained, having layers of sand, silt, and clay in different proportions. The KT deposits were evolved by a combination of two depositional environments, the glacio-fluvial at the base and the lacustrine at the top.

The mineral magnetic analysis reflects the dominance of detrital influx depicting warm episodes with well-oxygenated ponding conditions that ended with restricted cold climatic events. Palynological analysis show presence of pollen-spores of local terrestrial herbaceous as well as marshy taxa, along with temperate tree taxa transported from lower altitudes in good amount during Early Holocene. The carbon isotopic analysis shows that the GGR is characterized by both C_3-C_4 i.e. mixed type of vegetation. The average value in the weight % of BC is 0.07 and of $\delta^{13}C_{BC}$ is -25.2‰ which is close to atmospheric aerosols containing vehicular emissions mainly during the common traffic (~-26‰).

Tributary glaciers, snow-melt ephemeral streams, mass movements, landslide lake outburst flooding (LLOF) and glacier lake outburst flooding (GLOF) are important processes that modify the landforms and play an important role in the landscape evolution. The paraglacial processes affect the glacial signatures and creates confusion in the identification of landforms. This is the reason for different views of retreat and climate change for the same glacier.

The geochronology of various sections of the glacial stratified deposits provide the climate change of last 25 ka BP with major warm and cold events such as Last Glacial Maximum (21-19.5 Ka BP), Older Dryas (16.5-14.5 Ka BP), Bølling-Allerød (14.5-13.5 Ka BP), Younger Dryas (13.5-12 Ka BP), Indus Valley Civilization Collapse (5.0-3.0 Ka BP), Medieval Warm Period (1.25-0.7 Ka BP) and Little Ice Age (0.7-0.2 Ka BP).

The sequence of evolution of diversified landforms has helped in establishing the glacial stratigraphy for the first time, such as Terminal Moraines (62.89±8.58 Ka BP), Oldest Lateral Moraines (~ 60 Ka BP), Oldest Outwash Plains (~ 60 Ka BP), Kame Terraces (25.0 - 0.3 Ka BP), Old Lateral Moraines (17.56±4.11 - 4.84±1.21 Ka BP), Old Outwash Plains (5.13±1.54 - 3.3 Ka BP), Debris Cones (5.2-1.8 Ka BP), New Lateral Moraines (1.0 - 0.35 Ka BP) and New Outwash Plains (1.82 - 1.0 Ka BP).

ACKNOWLEDGEMENTS

REFERENCES

Ageta, Y., Naito, N., Nakawo, M., Fujita, K., Shankar, K., Pokhrel, A.P. and Wangda, D. 2001. Study project on the recent rapid shrinkage of summer-accumulation type glaciers in the Himalayas, 1997-1999. Bulletin of Glaciological Research, 18: 45-49.

Ali, S.N. and Juyal, N. 2013. Chronology of late quaternary glaciations in Indian Himalaya: a critical review. J. Geol. Soc. of India, 82: 628–638.

Alley, R.B., Meese, D.A., Shuman, C.A., Gow, A.J., Taylor, K.C., Grootes, P.M., White, J.W.C., Ram, M., Waddington, E.D., Maylewski, P.A. and Zielinski, G.A. 1993. Abrupt increase in Greenland snow accumulation at the end of the Younger Dryas event. Nature, 362: 527–529.

Armstrong, R.L. 2010. The Glaciers of the Himalayan-Hindu-Kush Region. Technical Paper. The International Centre for Integrated Mountain Development (ICIMOD), Kathmandu, Nepal.

Auden, J.B. 1937. Snout of the Gangotri glacier, Tehri Garhwal. Records of Geological Survey of India, 72/2: 135-140.

Bahuguna, I.M., Rathore, B.P., Brahmbhatt, R., Sharma, M., Dhar, S., Randhawa, S.S., Kumar, K., Romshoo, S., Shah, R.D., Ganjoo, R.K. and Ajai, 2014. Are the Himalayan glaciers retreating? Current Science, 106 (7): 1008-1013.

Bali, R., Agarwal, K.K., Ali, S.N. and Srivastava, P. 2011. Is the recessional pattern of Himalayan glaciers suggestive of anthropogenically induced global warming? Arabian Journal of Geosciences, 4 (7–8): 1087–1093.

Bali, R., Awasthi, D.D. and Tiwari, N.K. 2003. Neotectonic control on the geomorphic evolution of the Gangotri glacier Valley, Garhwal Himalaya. Gondwana Research, 6: 829–838.

Bali, R., Chauhan, M.S., Mishra, A.K., Ali, S.N., Tomar, A., Khan, I., Singh, D.S. and Srivastava, P. 2017a. Vegetation and climate change in the temperate-subalpine belt of Himachal Pradesh since 6300 cal. yrs. BP, inferred from pollen evidence of Triloknath palaeolake. Quaternary International , 444: 11–23.

Bali, R., Khan, I., Sangode S.J., Mishra, A.K., Ali, S.N., Singh, S.K., Tripathi, J.K., Singh, D.S. and Srivastava, P. 2017b. Mid- to late Holocene climate response from the Triloknath palaeolake, Lahaul Himalaya based on multiproxy data. Geomorphology, 284: 206–219.

Ballantyne, C.K. 2002. Paraglacial geomorphology. Quaternary Science Reviews 21: 1935–2017.

Barnard, P.L. Owen, L.A. and Finkel, R.C. 2004. Style and timing of glacial and paraglacial sedimentation in a monsoon-influenced high Himalayan environment, the upper Bhagirathi Valley, Garhwal Himalaya. Sedimentary Geology, 165(3–4): 199–221.

Benn, D.I. and Evans, D.J.A. 1998. Glaciers and Glaciations. Arnold, London, p. 734.

Benn, D.I. and Owen, L.A. 1998. The role of the Indian summer monsoon and the mid-latitude westerlies in Himalayan glaciation: review and speculative discussion. Geological Survey of India, 155 (2): 353–363.

Benn, D.I. and Owen, L.A. 2002. Himalayan glacial sedimentary environments: a framework for reconstructing and dating the former extent of glaciers in high mountains. Quaternary International, 97–98: 3–25.

Bhambri, R., Bolch, T. and Chaujar, R.K. 2012. Frontal recession of Gangotri glacier, Garhwal Himalayas, from 1965 to 2006 measured through high-resolution remote sensing data. Current Science 102: 489–494.

Bhattacharya A., Bolch T., Mukherjee K., King , O., Menounos, B., Kapitsa, V., Neckel, N., Yang, W. and Yao, T. 2021. High Mountain Asian glacier response to climate revealed by multi-temporal satellite observations since the 1960s. Nature Communications, 12:4133: 1-13. https://doi.org/10.1038/s41467-021-24180-y

Bhattacharya, A., Bolch, T., Mukherjee, K., Pieczonka, T., KropáčEk, J. and Buchroithner, M.F. 2016. Overall recession and mass budget of Gangotri glacier, Garhwal Himalayas, from 1965 to 2015 using remote sensing data. Journal of Glaciology, 62(236): 1115–1133.

Bohra, A., Kotlia, B.S. and Basavaiah, N. 2017. Palaeoclimatic reconstruction by using the varvite sediments of Bharatpur, upper Lahaul Valley, NW Himalaya, India. Quaternary International, 443(B): 39–48.

Bradley, R.S. 1992. When was the "Little Ice Age"? In: Mikami, T. (Ed.), Proceedings of the International Symposium on the Little Ice Age Climate. Tokyo Metropolitan University, Tokyo, 1-4.

Bradley, R.S. and Jones, P.D. 1993. Little Ice Age's summer temperature variations: their nature and relevance to recent global warming trends. The Holocene, 3: 367-376.

Chakraborty, S., Bhattacharyya, S. K., Ranhotra, P. S., Bhattacharyya, A. and Bhushan, R. 2006. Palaeoclimatic scenario during Holocene around Sangla valley, Kinnaur, northwest Himalaya based on multi proxy records. Current Science 91: 777–782.

Derbyshire, E., Li, J., Perrott, F.A., Xu, S. and Waters, R.S. 1984. Quaternary glacial history of the Hunza Valley, Karakoram Mountains, Pakistan. In: Miller, K. (Ed.), International Karakoram Project, Cambridge University Press, 456-495.

Dobhal, D.P, Gupta, A.K, Mehta, M. and Khandelwal, D.D. 2013. Kedarnath disaster: facts and plausible cause. Current Science, 105: 171–174

Dobhal, D.P., Pratap B., Bhambri R. and Mehta, M. 2021. Mass balance and morphological changes of Dokriani glacier (1992–2013), Garhwal Himalaya, India.Quaternary Science Advances, 4: 100033. https://doi.org/10.1016/j.qsa.2021.100033

Dubey, C.A., Singh, D.S., Singh, A.K., Sangode,S.J., Kumar, D. and Kumar P. 2022. Sedimentation pattern of kame terraces and its implication to climatic events in the Gangotri glacier region since 25 Ka BP, Garhwal Himalaya, India. Journal of Asian Earth Sciences, 229: 1- 9.https://doi.org/10.1016/j.jseaes.2022.105160

Evans, D.J.A., Owen, L. and Roberts A.D. 1995. Stratigraphy and sedimentology of Devensian (Dimlington Stadial) glacial deposits, east Yorkshire, England. Journal of Quaternary Science, 10: 241-265

Eyles, N., Eyles, C.H. and Miall, A.D. 1983. Lithofacies types and vertical profile models; an alternative approach to the description and environmental interpretation of glacial diamict and diamictite sequences. Sedimentology, 30: 393-410.

Faure, G. 1998. Principles and Applications of Inorganic Geochemistry (Second Edition). Prentice-Hall, Upper Saddle River, NJ. 8-21.

Fort, M. 1987. Sporadic morphogenesis in a continental subduction setting: An example from the Annapurna Range, Nepal Himala. Zeit far Geomorph., Suppl. Bd, 63: 9-36.

Fort, M. 1995. The Himalayan Glaciation: Myth and reality. Journal of the Nepal Geological Society, 11: 257-272.

Fujita, K., Suzuki, R., Nuimura, T. and Sakai, A. 2008. Performance of ASTER and SRTM DEMs, and their potential for assessing glacial lakes in the Lunana region. Bhutan Himalaya. Journal of Glaciology, 54: 220-228.

Fujita, K., Suzuki, R., Nuimura, T., Yamaguchi, S. and Sharma, R.R. 2009. Recent changes in Imja Glacial Lake and its damming moraine in the Nepal Himalaya revealed by in situ surveys and multi-temporal ASTER imagery. Environmental Research Letters, 4: 7, 045205.

Gantayat, P., Kulkarni, A.V. and Srinivasan, J. 2014. Estimation of ice thickness using surface velocities and slope: case study at Gangotri glacier, India. J. Glaciol., 60: 277–282.

Griesbach. C.L. 1891. Geology of the Central Himalayas. Geological Survey of India. Memoirs, 23: 27.

Groves, J.M. 1988. The Little Ice Age. Methuen, London, 498 PP.

GSI, 2009. Inventory of the Himalayan Glaciers. In: Sangewar, C.V., Shukla, S.P. and Singh, R.K. (Eds.), A Contribution to International Hydrological Programme, Geological Survey of India Special Publication No. 34.

Hewitt, K., 1993. Altitudinal organization of Karakoram geomorphic processes and depositional environments. Shroder, J.F. jr. (Eds.) Himalaya to the Sea, Geology, geomorphology and the Quaternary. Routledge Press, London: 159-183.

Hodgson, J.A. 1822. Journal of a survey to the heads of the rivers, Ganges and Jumna. Asiatic Research, 14: 60-152.

Houghton, J.T., Jenkins, G.T. and Ephraums, J 1990. Climate Change. In: J. (Eds.), The IPCC Scientific Assessment. Cambridge University Press, Cambridge.

Houghton, J.T., Meira Filho, L.G., Callander, B.A., Harris, N. and Kattenberg, A. 1996. Climate Change 1995, In :Maskell, K. (Eds.), The Science of Climate Change. Cambridge University Press, Cambridge.

Jangpangi, B.S. 1958. Study of some of the Central Himalaya glaciers, Journal of Science and Industrial Research Suppl., 17a(12): 91-93.

Juyal, N., Pant, R.K., Basavaiah, N., Bhushan, R., Jain, M., Saini, N.K., Yadava, M.G. and Singhvi, A.K. 2009. Reconstruction of Late Glacial to early Holocene monsoon variability from relict lake sediments of the Higher Central Himalaya, Uttrakhand, India. Journal of Asian Earth Science, 34: 437–449

Juyal, N., Sundriyal, Y.P., Rana, N., Chaudhary, S. and Singhvi, A.K. 2010. Late Quaternary fluvial aggradation and incision in the monsoon-dominated Alaknanda valley, Central Himalaya, Uttrakhand, India. Journal of Quaternary Science, 25(8): 1293–1304.

Kar, R. 2008. Palynological studies and geomorphological observation around Chaurabari glacier (Kedarnath): Interpretation of climatic changes and glacial fluctuations during Holocene (Abstract publication). In National Seminar on Glacial Geomorphology and Palaeoglaciation in Himalaya, Lucknow, 95–97.

Kar, R., Ranhotra, P. S., Bhattacharyya, A. and Sekar, B. 2002. Vegetation vis-à-vis climate and glacial fluctuations of the Gangotri glacier since the last 2000 years. Curr. Sci., 82: 347–351.

Kick, W. 1986. Glacier mapping for an inventory of the Indus drainage basin: current state and future possibilities. Ann. of Glacio., 8: 102–105.

Kohn, M. J. 2010. Carbon isotope compositions of terrestrial C_3 plants as indicators of (paleo) ecology and (paleo) climate, In: Proceedings of the National Academy of Sciences, 107(46): 19691-19695.

Kotlia, B.S., Sanwal, J., Phartiyal, B., Joshi, L.M., Trivedi, A. and Sharma, C. 2010. Late Quaternary climatic changes in the eastern Kumaun Himalaya, India, as deduced from multi-proxy studies. Quaternary International, 213 (1–2): 44–55.

Kotlia, B.S., Singh, A.K., Sanwal, J., Raza, W., Ahmad, S.M., Joshi, L.M., Sirohi, M., Sharma, A.K. and Sagar, N. 2016. Stalagmite inferred high resolution climatic changes through Pleistocene-Holocene Transition in Northwest Indian Himalaya. J. Earth Sci. Clim. Change, 7: 338. doi: 10.4172/2157-7617.1000338.

Kuhle, M. 1986. The upper limit of glaciation in the Himalayas. Geo. Journal, 13(4), 331–346.

Kuhle, M. 1997. New findings concerning the Ice Age (Last Glacial Maximum) glacier cover of the East-Pamir, of the Nanga Parbatup to the Central Himalaya and of Tibet, as well as the age of the Tibetan Inland Ice. Geo. Journal, 42: 87–257.

Kumar, D., Singh, A.K. and Singh, D.S. 2021a. Spatio-temporal fluctuations over Chorabari glacier, Garhwal Himalaya, India between 1976 and 2017. Quaternary International, 575–576: 178–189.

Kumar, D., Singh, A.K., Taloor, A.K. and Singh, D.S. 2021b. Recessional Pattern of Thelu and Swetvarn glaciers between 1968 and 2019 Bhagirathi basin, Garhwal Himalaya, India. Quaternary International, 575-576: 227-235.

Kumar, K., Dumka, R.K., Miral, M.S., Satyal, G.S. and Pant, M. 2008. Estimation of retreat rate of Gangotri glacier using rapid static and kinematic GPS survey. Current Science, 94 (2): 258–262.

Kumar, V., Mehta, M., Mishra, A. and Trivedi, A. 2017. Temporal fluctuations and frontal area change of Bangni and Dunagiri glaciers from 1962 to 2013, Dhauliganga Basin, central Himalaya, India. Geomorphology 284: 88–98.

Kumar, V., Shukla, T., Mishra, A., Kumar, A. and Mehta, M., 2020. Chronology and climate sensitivity of the post-LGM glaciation in the Dunagiri valley, Dhauliganga basin, Central Himalaya, India. Boreas, 49: 594–614.

Lange, O.L., Green, T.G.A. and Ziegler, H. 1988. Water status related photosynthesis and carbon isotope discrimination in species of the lichen genus Pseudocyphellaria with green or blue-green photo bionts and in photo sym bio demes. Oecologia 75:494–501.

Lee, S.Y., Seong, Y.B., Owen, L.A., Murari, M.K., Lim, H.S., Yoon, H.I. and Yoo, K.C. 2014. Late Quaternary glaciation in the Nun- Kun massif, north- western India. Boreas, 43 (1): 67–89.

Lee, Y.I., Lim, H.S. and Yoon, H.I. 2009. Carbon and nitrogen isotope composition of vegetation on King George Island, maritime Antarctic. Polar Biol. 32: 1607–1615. https://doi.org/10.1007/s00300-009-0659-5.

Leipe, C., Demske, D., Tarasov, P.E. and HIMPAC Project Members 2014. A Holocene pollen record from the northwestern Himalayan lake Tso Moriri: implications for palaeoclimatic and archaeological research. Quaternary International, 348: 93–112.

MacDonald, G. 2011. Potential influence of the Pacific Ocean on the Indian summer monsoon and Harappan decline. Quaternary International, 229: 140–148.

Madella, M. and Fuller D.Q. 2006. Palaeoecology and the Harappan civilisation of south Asia: a reconsideration. Quaternary Science Reviews, 25: 1283–1301.

Mayewski, P.A. and Jeschke, P.A. 1979. Himalayan and Trans-Himalayan glacier fluctuations since AD 1812. Arct. Alp. Res., 11: 267-287.

Mehta, M., Majeed, Z., Dobhal, D.P. and Srivastava, P., 2012. Geomorphological evidences of post-LGM glacial advancements in the Himalaya: A study from Chorabari glacier, Garhwal Himalaya, India. Journal of Earth System Science, 121 (1): 149–163.

Naithani, A.K., Nainwal, H.C., Sati, K.K. and Prasad, C. 2001. Geomorphological evidences of retreat of the Gangotri glacier and its characteristics. Current Science,80, 87–94.

Owen, L.A., Caffee, M.W., Finkel, R.C. and Seong, B.Y. 2008. Quaternary glaciations of the Himalaya-Tibetan orogen. Journal of Quaternary Science, 23: 513-532.

Owen, L.A., Derbyshire, E. and Fort, M. 1998. The Quaternary glacial history of the Himalaya. Journal Quaternary Science, 6: 91-120.

Owen, L.A., Finkel, R.C. and Caffee, M.W. 2002. A note on the extent of glaciation in the Himalaya during the global Last Glacial Maximum. Quaternary Science Reviews, 21: 147–158.

Phadtare, N.R. 2000. Sharp decrease in summer monsoon strength 4000-3500 cal yr B.P. in the central higher Himalaya of India based on pollen evidence from alpine peat. Quaternary Research, 53: 122–129.

Porter, S.C. 1970. Quaternary glacial record in Swat Kohistan, west Pakistan. Geological Society of America Bulletin, 81(5): 1421-1446.

Puri, V.M.K. 1984. Gangotri glacier-report on the Interdepartmental Expedition-1975. (Progress Report) Report to Geological Survey of India (Unpublished).

Puri, V.M.K. 1991. Report on survey of selected (Gangotri) glacier by terrestrial photogrammetry, district Uttarkashi, Uttar Pradesh (Progress Report) Report to Geological Survey of India (Unpublished).

Puri, V.M.K. and Singh, 1974. Report on Gangotri glacier. Report to Geological Survey of India (Unpublished).

Raina, V.K. 2009. Himalayan glaciers: a State-of-art Review of Glacial Studies, Glacial Retreat and Climate Change. Ministry of Environment and Forests, New Delhi, India.

Raina, V.K. 2013. Global warming and the glacier retreat: an overview. In: Sinha, Ravindra (Eds.), Earth System Processes and Disaster Management. Springer, 9-23.

Ranhotra, P. S., Bhattacharyya, A., Kar, R. and Sekar, B. 2001. Vegetation and climatic changes around Gangotri glacier during Holocene. Geological Survey of India, Spec. Publ, 65: 67–71.

Ranhotra, P.S. and Bhattacharyya, A. 2004. Vegetation, climate and lake history of Tapoban, Gangotri glacier, Garhwal Himalaya. Geological Survey of India, Spec. Publ., 80: 215–221.

Ranhotra, P.S. and Bhattacharyya, A. 2010. Holocene palaeoclimate and glacier fluctuations within Baspa Valley, Kinnaur, Himachal Pradesh. Geological Survey of India, 75: 527–532.

Ranhotra, P.S. and Kar, R. 2011. Palynological study of glaciogeomorphic features and its relevance to Quaternary palaeoclimate and glacial history. Current Science, 100: 641–647.

Rawat, S., Gupta, A.K., Sangode, S.J., Srivastava, P. and Nainwal, H.C. 2015. Late Pleistocene-Holocene vegetation and Indian summer monsoon record from the Lahaul, Northwest Himalaya, India. Quaternary Science Reviews, 114: 167–181.

Reading, H.G. 1986. Sedimentary Environments and Facies. Blackwell, London: 669.

Richards, B.W.M., Benn, D.I., Owen, L.A., Rhodes, E.J. and Spencer, J.Q. 2000. Timing of Late Quaternary glaciations south of Mount Everest in the Khumbu Himal, Nepal. Geo. Soc. of American Bul., 112: 1621–1632.

Ruddiman, W.F. and Kutzbach, J.E. 1991. Plateau uplift and climatic change. Scientific American, 264(3): 66-72.

Ryder, J.M. 1971. The stratigraphy and morphology of para-glacial alluvial fans in south-central British Columbia. Canadian Journal of Earth Science, 8 (2): 279-298.

Sangewar, C.V. 1997. Report on glacier front fluctuation in parts of H.P. and U.P. Geological survey of India, (Unpublished).

Sangode, S.J. and Bloemendal, J. 2004. Pedogenic transformation of magnetic minerals in Plio-Plestocene paleosols of the Siwalik Group, NW Himalaya, India. Paleogeography, Paleoclimatology, Paleoecology 212: 95–118.

Sangode, S.J., Mishra, S., Naik, S., and Deo, S. 2007. Magnetostratigraphy of the Quaternary sediments associated with some Toba tephra and Acheulian artefact bearing localities in the western and central India. Gondwana Magazine, 10: 111–121.

Sanwal, J., Kotlia, B.S., Rajendran, C., Ahmad, S.M., Rajendran, K. and Sandiford, M. 2013. Climatic variability in Central Indian Himalaya during the last ~1800 years: Evidence from a high resolution speleothem record. Quaternary International, 304: 183–192.

Sawlani, R., Agnihotri, R., Sharma, C., Patra, P.K., Dimri, A.P., Ram, K. and Verma, R.L. 2019. The severe Delhi SMOG of 2016: a case of delayed crop residue burning, coincident firecracker emissions, and atypical meteorology. Atmospheric Pollution Research,. 10: 868–879.

Saxena, A. and Singh D.S. 2017. Multiproxy records of vegetation and monsoon variability from the lacustrine sediments of eastern Ganga Plain since 1350 A.D. Quaternary International, 444 (A): 24–34.

Shankar, R. and Srivastava, D. 1999. Invited papers, Symp. Snow, Ice and Glaciers: A Himalayan Perspective, GSI, Lucknow, 9–11: 1–7.

Sharma, M.C. and Owen, L.A. 1996. Quaternary glacial history of NW Garhwal, Central Himalayas. Quaternary Science Reviews, 15(4): 335–365.

Singh, A.K., Kumar, D., Kumar, V. and Singh, D.S. 2020. Study of temporal response (1976–2019) and associated mass movement event (during 2017) of Meru glacier, Bhagirathi valley, Garhwal Himalaya, India. Quaternary International, 565: 12–21.

Singh, D.S. 2004. Late quaternary morpho-sedimentary processes in the Gangotri glacier area Garhwal Himalaya, India. Geological Survey of India, Spec. Pub. 80: 97–103.

Singh, D.S. 2013a. Snow melt ephemeral streams in the Gangotri glacier area, Garhwal Himalaya, India. In: Kotlia, B.S. (Eds.), Holocene: Perspectives, Environmental Dynamics and Impact Events. Nova Sci. Pub., USA,157–164.

Singh, D.S. 2013b. Causes of Kedarnath tragedy and human responsibilities. J. Geol. Soc. India, 82 (3): 303-304.

Singh, D.S. 2014. Surface Processes during flash floods in the glaciated terrain of Kedarnath, Garhwal Himalaya and their role in the modification of landforms. Current Science, 106(4): 594–597.

Singh, D.S. 2015. Climate Change: Past Present and Future. Geological Survey of India, 85: 634–635.

Singh, D.S. 2018. Concept of Rivers: An Introduction for Scientific and Socio- Economic Aspects.In: Singh, D.S. (Eds.), The Indian Rivers: Scientific and Socio-economic aspects. Springer publication, 1–24.

Singh, D.S. and Awasthi, A. 2011a. Implication of drainage basin parameters of Chhoti Gandak river, Ganga Plain, India. Geological Survey of India, 78(2): 370–378.

Singh, D.S. and Awasthi, A. 2011b. Natural hazards in the Ghaghara river area, Ganga Plain, India. Nat. Hazards. 57: 213–225.

Singh, D.S. and Mishra, A. 2001. Gangotri glacier characteristics, retreat and processes of sedimentation in the Bhagirathi valley. Geological Survey of India Spec. Pub, 65(3): 17–20.

Singh, D.S. and Mishra, A. 2002a. Role of tributary glaciers on landscape modification in the Gangotri glacier area, Garhwal Himalaya, India. Current Science, 82 (5): 101-105.

Singh, D.S. and Mishra, A. 2002b. Gangotri glacier System: an analysis using GIS technique. In: Pant, C.C., Sharma, A.K. (Eds.), Aspects of Geology and Environment of the Himalaya. Gyanoday Prakashan, Nainital, pp. 349-358.

Singh, D.S. and Ravindra, R. 2011a. Geomorphology of the MidreLoven glacier, Ny-Alesund, Svalbard, Arctic. In: Singh, D.S., Chhabra, N.L. (Eds.), Geological Processes and Climate Change Macmillan Publishers India Ltd. 269–281.

Singh, D.S. and Ravindra, R.. 2011b. Control of glacial and fluvial environments in the Ny- Alesund region. Arctic. Mausam, 62(4): 641–646.

Singh, D.S. and Singh, I.B. 2005. Facies Architecture of the Gandak Megafan, Ganga Plain, India. The Palaeontological Society of India, Spec. Pub., l2: 125–140.

Singh, D.S., Awasthi, A. and Bhardwaj, V. 2009. Control of tectonics and climate on Chhoti Gandak River Basin, East Ganga Plain. India. Himal. Geol., 30(2): 147–154.

Singh, D.S., Awasthi, A. and Nishat, R. 2010. Impact of Climate Change on the Rivers of Ganga Plain. Int. J. of Rural Develop. and Manage. Std., 4(1): 1–8.

Singh, D.S., Dubey, C.A., Kumar, D., Kumar, P. and Ravindra, R. 2018. Climate events between 47.5 and 1 ka BP in glaciated terrain of the Ny-Alesund region, Arctic, using geomorphology and sedimentology of diversified morphological zones. Polar Science, 18: 123–134.

Singh, D.S., Dubey, C.A., Kumar, D., Vishawakarma, B., Singh, A.K., Tripathi, A., Gautam, P.K., Bali, R., Agarwal, K.K. and Sharma, R. 2019. Monsoon variability and major climatic events between 25 and 0.05 ka BP using sedimentary parameters in the Gangotri glacier region, Garhwal Himalaya, India. Quaternary International, 507: 148–155.

Singh, D.S., Gupta, A.K., Sangode, S.J., Clemens, S.C., Srivastava, P., Prajapati, S.K. and Prakasam, M. 2015. Multiproxy record of monsoon variability from the Ganga Plain during 400-1200 A.D. Quaternary International, 371: 157–163.

Singh, D.S., Kumar, S., Kumar, D., Nishat, Awasthi, A. and Bhardwaj, V. 2013. Sedimentology and channel pattern of the Chhoti Gandak River, Ganga Plain, India. Gondwana Geological Magazine, 28(2): 171-180.

Singh, D.S., Tangri, A.K., Kumar, D., Dubey, C.A. and Bali, R. 2017. Pattern of retreat and related morphological zones of Gangotri glacier, Garhwal Himalaya, India. Quaternary International, 444 :172–181.

Singh, D.S., Dubey, C.A., Singh, A.K. and Ravindra, R. 2022. Geomorphology and Landscape Evolution of Ny-Alesund Region and Its Implication for Techtoniques, Svalbard, Arctic. In: Khare, N., (Eds.), Climate change in the Arctic. CRC Press, DOI:10.1201/9781003265177-5.

Singh, I.B., Srivastava, P., Sharma, S., Sharma, M., Singh, D.S., Rajgopalan, G. and Shukla, U. K. 1999. Upland interfluve (Doab) deposition: Alternative model to muddy over bank deposits. Facies, 40, 197-210.

Singh, J., Yadav, R.R., Negi, P.S. and Rastogi, T. 2020. Sub-alpine trees testify late 20th century rapid retreat of Gangotri glacier, Central Himalaya. Quaternary International, 565: 31–40.

Singh, P., Haritashya, U.K., Kumar, N. and Singh, Y. 2006. Hydrological characteristics of Gangotri glacier, Central Himalayas, India. Journal of Hydrology, 327(1-2): 55–67

Singh, V., Farooqui, A., Mehrotra, N.C., Singh, D.S., Tewari, R., Jha, N. and Kar, R. 2011. Late Pleistocene and early Holocene climate of Ny-Alesund, Svalbard (Norway): a study based on biological proxies. Journal of the Geological Society of India, 78 (2): 109–116.

Srivastava, D. 2012. Status Report on Gangotri Glacier, Science and Engineering Research Board, Department of Science and Technology, New Delhi, Himalayan Glaciology Technical Report No.3., 102 pp.

Srivastava, P., Agnihotri, R., Sharma, D., Meena, N., Sundriyal, Y. P., Saxena, A., Bhushan, R., Sawlani, R., Banerji, U.S., Sharma, C., Bisht, P., Rana, N. and Jayangondaperumal, R. 2017. 8000-year Monsoonal Record from Himalaya Revealing Reinforcement of Tropical and Global Climate Systems since Mid-Holocene. Scientific Reports, 7: 14515. doi:10.1038/s41598-017-15143-9.

Srivastava, P., Singh, I.B., Sharma, S., Shukla, U.K. and Singhvi, A.K., 2003. Late Pleistocene-Holocene hydrologic changes in the interfluve areas of the central Ganga Plain, India. Geomorphology, 54(3): 279–292.

Tangri, A.K., 2002. Shrinking glaciers of Uttaranchal; cause of concern and hope for the future. In: Pant, C.C., Sharma, A.K. (Eds.), Aspects of Geology and Environment of the Himalaya. Gyanoday Prakashan, Nainital, 359-367.

Tangri, A.K., Chandra, R. and Yadav, S.K.S., 2004. Temporal monitoring of the snout, equilibrium line and ablation zone of Gangotri glacier through remote sensing and GIS techniques - an attempt at deciphering the climatic variability. In Srivastava, D., Gupta, K.R. and Mukerji, S.(Editors), Geological Survey of India Special Publication, 80: 145-153.

Trivedi, A., Singh, D.S., Chauhan, M.S., Arya, A., Bhardwaj, V. and Awasthi, A. 2011. Vegetation and climate change around Ropan Chhappra Tal in Deoria District, The Central Ganga Plain During the Last 1350 Years. The Palaeontological Society of India, 56(1): 39–43.

Vohra, C.P. 1988. Gangotri glacier. Indian Mountaineer, Indian Mountaineering Foundation, 1-8.

Vohra, C.P., 1971. Report of the Training-Cum- Study Expedition to the Gangotri glacier. INCH, CSIR, New Delhi.

Yadav, R.R., Park, W.K., Singh, J. and Dubey, B. 2004. Do the western Himalayas defy global warming? Geophysical Research Letters 31, L17201. http://dx.doi.org/ 10.1029/2004gl020201.

Yang, B., Brauning, A. and Shi, Y. 2003. Late Holocene temperature fluctuations on the Tibetan Plateau. Quaternary Science Reviews, 22: 2335–2344.

Zheng, B. and Rutter, N. 1998. On the problem of the Quaternary glaciations, and the extent and patterns of pleistocene ice cover in the Qinghaie Xizang (Tibet) plateau. Quaternary International 45 (46): 109-122.